

Date of publication xxxx 00, 0000, date of current version xxxx 00, 0000.

Digital Object Identifier 10.1109/ACCESS.2024.0429000

S5-SHB Agent: Society 5.0 enabled Multi-model Agentic Blockchain Framework for Smart Home

JANANI RANGILA¹, (Student, IEEE), AKILA SIRIWEERA², (Member, IEEE), INCHEON PAIK², (Senior Member, IEEE), KEITARO NARUSE², (Member, IEEE), ISURU JAYANADA¹, (Student, IEEE), and VISHMIKA DEVINDI¹, (Student, IEEE)

¹The KD University, Rathmalana, Colombo, Sri Lanka (e-mail: 40-bis-0019@kdu.ac.lk, 40-ict-0004@kdu.ac.lk, and 40-bis-0011@kdu.ac.lk)

²The University of Aizu, Aizu Wakamatsu, Japan (e-mail: asiriwe@u-aizu.ac.jp, paikic@u-aizu.ac.jp, and naruse@u-aizu.ac.jp)

Corresponding author: Akila Siriweera (e-mail: asiriwe@u-aizu.ac.jp).

Source code is available under the MIT License at <https://github.com/AsiriweLab/S5-SHB-Agent>.

arXiv:2603.05027v1 [cs.AI] 5 Mar 2026

ABSTRACT The smart home is a key application domain within the Society 5.0 vision for a human-centered society. As smart home ecosystems expand with heterogeneous IoT protocols, diverse devices, and evolving threats, autonomous systems must manage comfort, security, energy, and safety for residents. Such autonomous decision-making requires a trust anchor, making blockchain a preferred foundation for transparent and accountable smart home governance. However, realizing this vision requires blockchain-governed smart homes to simultaneously address adaptive consensus, intelligent multi-agent coordination, and resident-controlled governance aligned with the principles of Society 5.0. Existing frameworks rely solely on rigid smart contracts with fixed consensus protocols, employ at most a single AI model without multi-agent coordination, and offer no governance mechanism for residents to control automation behaviour. To address these limitations, this paper presents the Society 5.0-driven human-centered governance-enabled smart home blockchain agent (S5-SHB-Agent). The framework orchestrates ten specialized agents using interchangeable large language models to make decisions across the safety, security, comfort, energy, privacy, and health domains. An adaptive PoW blockchain adjusts mining difficulty based on transaction volume and emergency conditions, with digital signatures and Merkle tree anchoring to ensure tamper-evident auditability. A four-tier governance model enables residents to control automation through tiered preferences from routine adjustments to immutable safety thresholds. Evaluation confirms that resident governance correctly separates adjustable comfort priorities from immutable safety thresholds across all tested configurations, while adaptive consensus commits emergency blocks in under 10 ms. Across four interchangeable LLM variants, the multi-agent system sustains 100% decision acceptance with agent confidence consistently above 0.82 under both normal and threat operating conditions.

INDEX TERMS Agentic AI, Adaptive Consensus, Blockchain, Human-Centered Governance, IoT Security, Multi-Agent Systems, Smart Home, Society 5.0

I. INTRODUCTION

THE Japanese Cabinet Office's vision for Society 5.0 describes a human-centered society that integrates cyber and physical systems to improve social well-being alongside economic progress [1]–[3]. The smart home is the primary residence where people interact with interconnected devices for security, energy management, health monitoring, and indoor climate control [4], [5]. As these ecosystems expand, bridging heterogeneous device protocols and an ever-shifting threat landscape, the research community requires frameworks that govern such environments autonomously while remaining transparent and aligned with human values [3]–[5].

Blockchain technology has been widely applied to IoT security, offering cryptographic non-repudiation, tamper-evident logging, and decentralized consensus across domains ranging from smart home intrusion detection and healthcare to smart grids, smart cities, and general IoT infrastructure [5]–[12]. While these works demonstrate that blockchain can secure device transactions and audit logs, they treat consensus as a fixed parameter, AI as a single isolated model, and resident interaction as an access control problem, leaving the deeper challenge of human-centered, adaptive, multi-agent governance unaddressed [13]–[16].

Despite these efforts, a systematic review of recent

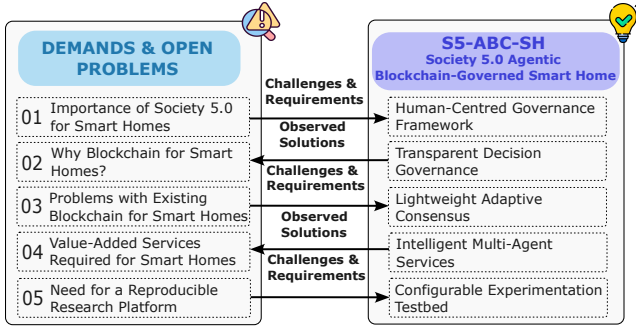


FIGURE 1: Gap-driven design motivation for S5-SHB-Agent

blockchain-based IoT frameworks [7]–[27] reveals five research gaps that prevent existing solutions from fulfilling Society 5.0’s human-centered vision: First, Society 5.0’s human-centered framing finds no counterpart in existing work. All surveyed works treat blockchain as purely technical infrastructure without considering how residents should retain agency over automation decisions. Current frameworks offer at best basic access control [8], [10], [18] with no tiered governance for resident-controlled preferences.

Second, all surveyed frameworks employ fixed consensus protocols incapable of runtime adaptation. Whether using Proof-of-Work [7], [9], Proof-of-Stake, Proof-of-Authority, or DAG/Tangle variants [20], thus resulted in static difficulty regardless of workload dynamics. This creates a mismatch in which routine telemetry logging coexists with safety-critical emergency commands that require rapid confirmation.

Third, LLM-based multi-agent orchestration is entirely absent from the surveyed landscape. The rigid reliance on smart contracts resulted in: pre-compiled contract logic encodes fixed rules that cannot reason across existing domain events. A smoke alarm and a power surge occurring simultaneously demand contextual judgment that no deterministic condition can encode. One of the AI integrations found is hybrid double Q-learning with Bi-LSTM [13], while others employ individual deep learning models [9], [12], [19] or metaheuristic optimization [20], [25]. LLM reasoning and cross-domain agent coordination across safety, security, energy, and health remain unexplored throughout. Furthermore, a single fixed model cannot simultaneously meet the sub-second response requirements of safety-critical agents and cost constraints of routine automation; tier-constrained multi-model routing is specifically designed to address heterogeneity.

Fourth, resident-controlled governance remains undifferentiated across all surveyed works. Existing governance is limited to consortium membership [8], encryption-gated access [18], or interoperability-level permissions [10]. Governance is uniformly flat; no tier structure separates resident-adjustable comfort settings from immutable safety thresholds.

Fifth, no framework offers user-selectable multi-mode deployment spanning simulation, real, and hybrid environments. The majority of surveyed works use simulation-only evaluation. Only [22] employs a real testbed and [17] com-

TABLE 1: Summary of Notation

Symbol	Definition
δ_t	Mining difficulty at block t
\bar{v}_t	Avg. transaction count over sliding window of w blocks
\mathcal{A}	Set of specialized agents $\{a_1, a_2, \dots, a_n\}$
$\mathcal{T}(t)$	Device telemetry vector at time t
$\pi(a_i)$	Continuous priority score of agent a_i
σ_i	Role-specific system prompt for agent a_i
$\tau(m_j)$	Capability tier of model m_j
\mathcal{R}	Tier-constrained model routing function
\mathcal{CR}	Four-level conflict resolution cascade
$\mathcal{S}(a)$	Composite ML score for agent a
\mathcal{G}	Governance tier set $\{\Gamma_1, \Gamma_2, \Gamma_3, \Gamma_4\}$
ϕ	Governance authorization function
\mathcal{M}_r	Merkle root over off-chain records

bines simulation with FPGA testing, but neither offers a unified platform with user-selectable mode switching. Fig. 1 illustrates how these five demands map to solution components in S5-SHB-Agent.

To address these gaps, we present the Society 5.0 Agentic Blockchain-Governed Smart Home (S5-SHB-Agent), built on three architectural layers. The Control Plane manages external interfaces and enforces governance policies. The Agent Intelligence layer coordinates 10 specialized AI agents (seven domains, three extensions) via a multi-model LLM router with tier-constrained provider assignment and a four-level conflict-resolution. The Device & Data layer abstracts IoT hardware through the Model Context Protocol alongside blockchain-anchored trust infrastructure. An adaptive Proof-of-Work blockchain scales mining difficulty with transaction volume. Firmware-level emergency bypass keeps safety commands instantaneous; Ed25519 digital signatures and Merkle anchoring produce unforgeable audit records. A four-tier governance model enables residents to shape automation, from daily comfort preferences to immutable safety thresholds, without requiring configuration expertise.

Our key contributions are:

- A four-tier human-centered governance model aligned with Society 5.0; residents control automation through routine adjustments, advanced overrides, and immutable safety thresholds via natural-language interfaces.
- A multi-agent orchestration architecture coordinating ten specialized AI agents across four priority tiers through a multi-model LLM router supporting four providers with tier-constrained model assignment.
- An adaptive PoW blockchain that adjusts mining difficulty based on transaction volume, complemented by firmware-level emergency bypass for immediate safety-critical response, with Ed25519 digital signatures and Merkle tree anchoring for tamper-evident auditability.
- A four-level conflict resolution resolving inter-agent disputes through safety override, LLM-based contextual arbitration, ML-based historical scoring, and priority-based fallback.
- A multi-mode deployment framework supporting simulation, real, and hybrid environments with a unified orchestration layer and tamper-evident Merkle anchoring.

TABLE 2: Grouped Comparison of Blockchain-Based IoT Framework Capabilities

References	Application Domain					Blockchain			AI / ML Integration						Human-Center Govern				Deployment Mode				
	SH	SG	HC	CE	SC/IoT	Fixed	Adapt	Cross	None	ML	Deep	RL	LLM	MultiA	MultiM	None	BAC	TierGov	S5.0	Sim	Real	Hybrid	Multi
G1: [7]–[9]	✓	-	-	-	-	✓	-	-	[8]	-	[7], [9]	-	-	-	-	[7], [9]	[8]	-	-	✓	-	-	-
G2: [10]	✓	-	✓	-	-	✓	-	✓	-	-	✓	-	-	-	-	-	✓	-	-	✓	-	-	-
G3: [11], [12], [17]	-	✓	-	-	-	✓	-	-	[11]	[17]	[12]	-	-	-	-	✓	-	-	-	✓	✓	-	-
G4: [13]–[16]	-	-	-	✓	-	✓	-	-	-	✓	✓	-	-	-	-	✓	-	-	-	✓	-	-	-
G5: [18], [19]	-	-	✓	-	-	✓	-	-	-	-	✓	-	-	-	-	[19]	[18]	-	-	✓	-	-	-
G6: [20]–[25]	-	-	-	-	✓	✓	-	-	[21], [22]	[20], [23]–[25]	-	-	-	-	-	✓	-	-	-	✓	✓	-	-
G7: [26], [27]	-	-	-	-	✓	✓	-	-	✓	-	-	-	-	-	-	✓	-	-	-	✓	-	-	-
Ours	✓	-	-	-	-	-	✓	✓	-	-	✓	-	✓	✓	✓	-	-	✓	✓	✓	✓	✓	✓

To the best of our knowledge, S5-SHB-Agent is the first smart-contract-free blockchained agentic framework that simultaneously addresses Society 5.0 framing, adaptive consensus, multi-agent multi-model LLM orchestration, tiered human-centered governance, and multi-mode deployment (simulation, real, and hybrid) for smart home IoT.

Table I outlines the summary of the notation table. The remainder of the paper is structured as follows. Section II reviews related work. Section III outlines preliminaries, including the motivation scenario and problem formulation. Section IV presents the proposed S5-SHB-Agent framework. Section V discusses system evaluation. Section V presents conclusion. Section VI concludes with future work.

II. RELATED WORKS

This section surveys twenty-one recent blockchain-based IoT publications from 2025 [7]–[27] spanning smart homes, smart grids, healthcare, consumer electronics, and general IoT security. We conducted a structured survey aligned with the research objective: *investigating the holistic, inclusive, and intelligent features that accommodate Society 5.0’s human-centered, agentic, and trust-anchored research paradigm for blockchain-enabled smart-home IoT*. The resulting taxonomy captures three dimensions: *holistic* (application domain coverage), *inclusive* (blockchain architecture, AI/ML integration depth, and human-centered governance), and *agile* (deployment mode flexibility). Table II presents the grouped comparison across these dimensions.

We identified seven groups (G1-G7) based on distinctive capability patterns. G1: [7]–[9] addresses smart home security using fixed consensus blockchains with traditional ML and deep learning, limited to simulation-only deployment. G2: [10] uniquely bridges smart home and healthcare domains through the only cross-chain interoperable architecture in the survey, with tiered access control but simulation-only evaluation. G3: [11], [12], [17] targets smart grid energy management combining traditional ML, metaheuristics, and deep learning; notably, [17] provides one of only two real-testbed validations across all surveyed works. G4: [13]–[16] exhibits the most sophisticated single-framework AI, uniquely combining deep learning with reinforcement learn-

ing (hybrid Double Q-Learning and Bi-LSTM in [13]) and quantum-assisted techniques in [16], though confined to fixed consensus and simulation-only deployment.

G5: [18], [19] applies blockchain to healthcare IoT with deep learning and encryption-based access control. G6: [20]–[25], the largest cluster, spans general IoT optimization and security; [22] provides the second real-testbed validation alongside simulation. G7: [26], [27] addresses smart city security with lightweight fixed-consensus blockchains and traditional ML. Despite progressive domain-specific advances, all seven groups share critical limitations: fixed consensus protocols, single-model AI at best, basic or absent governance, and predominantly simulation-only evaluation.

Five systematic research gaps emerge across all 21 works: (1) no Society 5.0 human-centered socio-technical framing, (2) no tiered governance enabling resident-controlled preferences, (3) no adaptive consensus capable of runtime difficulty adjustment, (4) no multi-agent LLM orchestration for intelligent conflict resolution, and (5) no user-selectable multi-mode deployment spanning simulation, real, and hybrid environments. Our proposed S5-ABC-HS-Agent addresses all five gaps simultaneously: adaptive PoW consensus adjusting difficulty based on transaction volume, 10 specialized AI agents with multi-model LLM routing across four providers (Google Gemini, Anthropic Claude, OpenAI GPT, local Ollama), four-tier Society 5.0 governance with immutable safety invariants, and unified multi-mode deployment with tamper-evident Merkle anchoring capabilities absent from every surveyed framework.

III. PRELIMINARY

This section introduces the motivation scenario and problem formulation. Section III-A presents a smart-home scenario that motivates the need for an agentic, blockchain-anchored, human-centered management system. Section III-B formulates six key challenges that drive our architectural contributions, and their mapping to solutions is shown in Figure 1.

A. SMART HOME GOVERNANCE SCENARIO

Smart residence, *Aizu-Residence*, is equipped with 16 IoT devices across ten categories: thermostats, door locks, smart lights, smoke sensors, gas sensors, motion sensors, security

cameras, smart plugs, HVAC systems, and smart appliances. The residence serves a family of four with differing preferences: an elderly occupant prioritizes safety and health monitoring, working adults balance energy efficiency with comfort, and a teenager favors entertainment automation and privacy. Devices generate continuous telemetry streams while multiple autonomous AI agents must collaboratively manage comfort, security, energy, and safety objectives in real time.

Aizu-Residence must address three governance concerns aligned with Society 5.0 human-centered principles. First, ensuring *trustworthy autonomy* through cryptographically verifiable decision-making, in which every agent action is digitally signed, validated, and immutably recorded, thereby eliminating opaque "black-box" automation. Second, guaranteeing *conflict-safe operation* when multiple agents issue contradictory commands on the same device, requiring intelligent resolution that always preserves occupant safety above all other objectives. Third, supporting *democratic governance* where residents, regardless of technical expertise, can meaningfully control automation behavior through tiered preferences, rather than being passive recipients of algorithmically determined outcomes.

Therefore, Aizu-Residence requires a framework that addresses trust (blockchain-anchored agent accountability with tamper-evident decision logs), intelligence (multi-agent orchestration with conflict resolution backed by multi-model LLM reasoning), and governance (a tiered human-centered preference model that ensures occupant autonomy remains paramount while safety constraints remain inviolable).

B. PROBLEM DEFINITION

We identify six critical challenges in blockchain-enabled agentic smart home IoT, each motivating a corresponding design component.

Definition 1 (Adaptive Consensus for IoT Transaction Throughput): Blockchain-based smart home systems generate heterogeneous transaction workloads ranging from routine telemetry logging to safety-critical emergency commands. Let δ_t denote the mining difficulty at block t and \bar{v}_t the average transaction count over a sliding window of w most recent blocks:

$$\bar{v}_t = \frac{1}{w} \sum_{i=t-w+1}^t |TX_i| \quad (1)$$

Fixed consensus protocols universally adopted by all 21 surveyed works impose static difficulty regardless of workload dynamics, causing either excessive latency during transaction bursts or wasted computation during idle periods. An adaptive consensus mechanism must dynamically adjust difficulty through stepwise clamped adjustment:

$$\delta_{t+1} = \begin{cases} \max(\delta_{\min}, \delta_t - 1), & \text{if } \bar{v}_t \geq v_{\text{high}} \quad (\text{high volume}) \\ \min(\delta_{\max}, \delta_t + 1), & \text{if } \bar{v}_t \leq v_{\text{low}} \quad (\text{idle period}) \\ \delta_t \rightarrow \delta_{\text{base}}, & \text{otherwise} \quad (\text{normal operation}) \end{cases} \quad (2)$$

where δ_{\min} and δ_{\max} are safety-bounded difficulty limits, v_{high} and v_{low} are transaction volume thresholds delineating operational regimes, and δ_{base} is the baseline difficulty toward which the system gravitates under normal conditions via stepwise increment or decrement. Emergency conditions (smoke, gas, intrusion) naturally produce high transaction volumes that trigger the $\bar{v}_t \geq v_{\text{high}}$ branch, lowering mining difficulty for faster block confirmation. This challenge motivates our adaptive PoW blockchain with safety-bounded difficulty range $[\delta_{\min}, \delta_{\max}] = [1, 4]$, base difficulty $\delta_{\text{base}} = 2$, volume thresholds $v_{\text{low}} = 3$ and $v_{\text{high}} = 10$, sliding window $w = 3$ blocks, and Ed25519 digital signatures for every agent transaction with full difficulty adjustment auditability.

Definition 2 (Multi-Agent Decision Orchestration): Smart home environments require simultaneous reasoning across multiple competing objectives safety, security, comfort, energy efficiency, privacy, and health that cannot be adequately addressed by single-model AI approaches. Let $\mathcal{A} = \{a_1, a_2, \dots, a_n\}$ denote the set of specialized agents, $\mathcal{T}(t)$ the device telemetry vector at time t , and $\pi : \mathcal{A} \rightarrow [0, 1]$ a priority function mapping agents to continuous priority scores. A multi-agent orchestration framework requires each agent to independently reason over telemetry and produce typed action commands:

$$a_i : \mathcal{T}(t) \xrightarrow{LLM_i(\sigma_i)} (cmd_i, conf_i), \quad conf_i \in [0, 1] \quad (3)$$

where LLM_i denotes the language model assigned to agent a_i , σ_i is the role-specific system prompt encoding domain expertise, cmd_i is the structured action command, and $conf_i$ is the confidence score. This challenge motivates our ten specialized AI agents organized across four priority tiers: Tier 1 Safety-Critical (Safety at $\pi = 1.0$, Health at $\pi = 0.9$), Tier 2 Security (Security at $\pi = 0.8$, Privacy at $\pi = 0.7$), Tier 3 Comfort (Energy at $\pi = 0.6$, Climate at $\pi = 0.5$, Maintenance at $\pi = 0.4$), and Tier 4 Specialized (NLU at $\pi = 0.85$, Anomaly at $\pi = 0.88$, Arbitration at $\pi = 0.95$), with each decision cryptographically signed and submitted to the blockchain.

Definition 3 (Multi-Model LLM Routing with Tier Constraints): Different agent responsibilities demand different levels of AI capability-safety-critical agents require the most capable models, routine agents can use cost-efficient alternatives, and privacy-sensitive deployments may require local inference. Let $\mathcal{P} = \{p_1, \dots, p_s\}$ denote LLM providers and $\mathcal{M} = \{m_1, \dots, m_q\}$ denote available models, each characterized by a capability tier $\tau(m_j) \in \{\text{flash}, \text{pro}\}$, a cost rate $c(m_j)$, and a privacy mode $\rho(m_j) \in \{\text{cloud}, \text{local}\}$. A tier-constrained model router must enforce:

$$\mathcal{R} : (a_i, \pi(a_i)) \rightarrow m_j, \quad \text{s.t. } \tau(m_j) \geq \tau_{\min}(\pi(a_i)) \quad (4)$$

where $\tau_{\min}(\pi(a_i))$ defines the minimum model tier required for the agent's priority level, ensuring safety-critical agents are always routed to `pro`-tier models. This challenge motivates our Model Router supporting four LLM providers (Google Gemini, Anthropic Claude, OpenAI GPT, and local

Ollama) with seven registered models across two capability tiers, per-agent tier constraint enforcement, four governance presets (balanced, max-privacy, budget, best-quality), and per-call cost and latency tracking logged to the off-chain model usage table.

Definition 4 (Intelligent Conflict Resolution): When multiple agents independently reason over shared device state, conflicting commands inevitably arise. Let cmd_i and cmd_j be conflicting commands from agents a_i and a_j targeting the same device d_k , where a conflict exists when both target the same device with different actions. A conflict resolution mechanism must deterministically resolve disputes while preserving safety invariants through a prioritized cascade:

$$\mathcal{CR}(cmd_i, cmd_j, d_k) = \begin{cases} cmd_s, & \text{L1} \\ \mathcal{L}(cmd_i, cmd_j, ctx), & \text{L2} \\ \arg \max_{a \in \{a_i, a_j\}} \mathcal{S}(a), & \text{L3} \\ \arg \max_{a \in \{a_i, a_j\}} \pi(a), & \text{L4} \end{cases} \quad (5)$$

where cmd_s is the safety agent's command (always wins at L1, architecturally immutable), \mathcal{L} denotes LLM-based contextual arbitration at L2, $\mathcal{S}(a) = 0.6 \cdot s_{ML}(a) + 0.4 \cdot \pi(a)$ is the composite ML score at L3 where $s_{ML}(a) = r_{accept} \cdot (1 - 0.5 \cdot r_{conflict})$ derives from historical acceptance and conflict rates, and L4 selects the highest-priority agent as fallback. This challenge motivates our Arbitration Agent implementing the four-level cascade with every conflict record and resolution outcome logged to off-chain storage and anchored on-chain.

Definition 5 (Human-Centered Tiered Governance): Society 5.0 principles demand that technology serves human agency rather than replacing it. Let $\mathcal{G} = \{\Gamma_1, \Gamma_2, \Gamma_3, \Gamma_4\}$ denote governance tiers with monotonically increasing impact and correspondingly decreasing mutability, and \mathcal{P}_u the preference set of resident u . A human-centered governance model must enforce tier-stratified preference control:

$$\phi(\mathcal{P}_u, \Gamma_k) = \begin{cases} allow, & \text{if } k \leq 3 \text{ and } \text{Valid}(g_i, v_{new}) \\ deny, & \text{if } k = 4 \text{ (immutable)} \end{cases} \quad (6)$$

where each preference change for $k \leq 3$ is subject to typed validation $\text{Valid}(g_i, v_{new}) = \text{TypeCheck}(v_{new}, \tau_i) \wedge \text{RangeCheck}(v_{new}, [\ell_i, u_i])$, and Tier 4 parameters satisfy the immutability invariant $\forall g_j \in \Gamma_4, \forall t : g_j(t) = g_j(t_0)$. Tier 1 (Γ_1) covers 8 safe adjustment keys (temperature, brightness, quiet hours, voice settings, alert filtering, daily reports), Tier 2 (Γ_2) manages 7 impactful trade-off keys (comfort-vs-energy balance, security-vs-privacy balance, anomaly sensitivity, automation level, confirmation mode, arbitration mode, anomaly training cycles), Tier 3 (Γ_3) permits 3 advanced override keys (per-agent device overrides, monthly API budget, allowed LLM providers), and Tier 4 (Γ_4) enforces 9 locked safety invariants (safety priority at 1.0, firmware gas threshold at 50 ppm, smoke threshold at 0.3, safety override immunity, Ed25519 key management, blockchain validation, minimum active detectors,

safety model minimum tier, and governance change logging). All changes are validated against 12 typed range-and-choice rules, logged on-chain as governance transactions, and Tier 4 parameters are computationally enforced as immutable. Residents interact through a natural language interface that translates voice and text commands into preference changes, enabling non-technical occupants to exercise meaningful control.

Definition 6 (Multi-Mode Deployment with Tamper-Evident Anchoring): Practical smart home research requires flexible evaluation across simulation, real hardware, and hybrid configurations with verifiable data integrity. Let $\mathcal{O} = \{\text{sim}, \text{real}, \text{hybrid}\}$ denote deployment modes, \mathcal{D}_{off} the off-chain data store, and M_r the Merkle root computed over batched off-chain records. Among surveyed works, only two achieve partial hybrid deployment [17], [22]; none offer user-selectable mode switching. A unified deployment framework must support seamless mode transitions through protocol-agnostic adapter abstraction with tamper-evident anchoring:

$$\mathcal{E}(d_j, \alpha, \theta) = \begin{cases} \text{MockAdapter}(d_j, \alpha, \theta), & \omega = \text{sim} \\ \text{ProtocolAdapter}(d_j, \alpha, \theta), & \omega = \text{real} \\ \text{Router}(d_j) \rightarrow \mathcal{E}, & \omega = \text{hyb} \end{cases} \quad (7)$$

where $\text{ProtocolAdap} \in \{\text{MQTTAdap}, \text{HTTPAdap}\}$ is selected based on device connection configuration, and hybrid mode independently routes each device to its designated adapter. The orchestrator operates identically across modes, producing blockchain-anchored records with Merkle root commitments $M_r = \text{MerkleRoot}(\{H(t_1), \dots, H(t_k)\})$ for tamper detection regardless of origin. This challenge motivates our orchestration layer coordinating telemetry collection via a bridge, off-chain SQLite storage across 13 tables (telemetry streams, reasoning logs, Merkle anchors, conflict records, decision outcomes, MCP health, NLU conversations, anomaly detections, arbitration logs, governance changes, and model usage), agent reasoning cycles, four-level conflict resolution, and mining with Merkle anchoring supporting three deployment modes via MQTT (QoS-1, optional TLS), HTTP (bearer/basic/API-key authentication), and Mock (per-device-type state simulation) adapters, a unified backend, and five WebSocket streams for real-time event updates.

IV. PROPOSED METHOD: S5-SHB-AGENT

This section presents the S5-HSB-Agent designed to address the six challenges identified in Section III. Section IV-A presents the reference architecture (RA). Section IV-B-B describes the system architecture (SA). Sections IV-C through IV-H detail the solutions addressing each problem definition.

A. REFERENCE ARCHITECTURE (RA) FOR S5-SHB-AGENT

Fig. 2 presents the RA of the S5-SHB Agent, organized into three primary layers: Control Plane, Agent Intelligence, and Device & Data, interconnected through defined communication channels. The layered design enforces separation of concerns: the Control Plane manages external interactions and

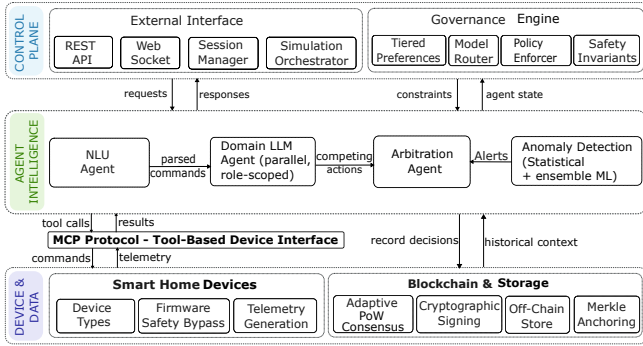


FIGURE 2: Reference architecture of S5-SHB Agent showing the three-layer design with Control Plane, Agent Intelligence, and Device & Data layers.

governance policies, the Agent Intelligence layer houses autonomous reasoning and conflict resolution, and the Device & Data layer encapsulates physical device abstraction alongside blockchain-anchored trust infrastructure. A Model Context Protocol (MCP) interface provides standardized tool-based device access between the Agent Intelligence and Device & Data layers in simulation mode, while a protocol adapter pattern (MQTT, HTTP) provides the same interface in real-device mode. This architecture directly instantiates the holistic (multi-domain coverage), inclusive (adaptive blockchain, multi-agent AI, tiered governance), and agile (multi-mode deployment) taxonomy dimensions established in Section II.

1) Control Plane

The Control Plane comprises two subsystems: the External Interface and the Governance Engine. The External Interface exposes the system through four components: a REST API for stateless request-response interactions, a WebSocket for bidirectional real-time streaming, a Session Manager for maintaining user context, and a Simulation Orchestrator for coordinating the operational loop across deployment modes. The Governance Engine enforces Society 5.0 human-centered principles through four components: Tiered Preferences, which manage the four-tier resident preference hierarchy; Model Router, which controls multi-provider LLM assignment with tier constraints; Governance Contract, which validates and logs all preference changes; and Safety Invariants, which enforce immutable Tier 4 safety thresholds that no agent or resident can override.

The Control Plane communicates downward through *requests* and receives *responses*, while the Governance Engine supplies *constraints* to agents and receives *agent state* updates, ensuring that agent reasoning always operates within resident-defined governance boundaries.

2) Agent Intelligence Layer

The Agent Intelligence layer implements the cognitive core through four functional components. The NLU Agent parses natural language voice and text commands into structured device actions with conversation context maintenance and

pronoun resolution. Parsed commands flow to the Domain LLM Agents a pool of parallel, role-scoped specialized agents (Safety, Health, Security, Privacy, Energy, Climate, Maintenance) that independently reason over device telemetry using provider-specific LLM calls with role-specific system prompts. When Domain LLM Agents produce competing actions targeting the same device, conflicts are forwarded to the Arbitration Agent, which implements the four-level resolution cascade (safety override, LLM arbitration, ML scoring, priority fallback) to deterministically resolve disputes.

The Anomaly Detection subsystem operates alongside the agent pipeline using statistical and ensemble ML methods Isolation Forest for multivariate outlier detection, Local Outlier Factor (LOF) for density-based anomaly identification, Z-score for univariate threshold monitoring, and an optional PyTorch autoencoder trained on normal telemetry patterns deliberately not LLM-based to detect telemetry anomalies and feed alerts directly to the Arbitration Agent. This separation ensures anomaly detection remains operational even when LLM providers are unavailable.

3) Device Access Interface

The device access layer provides two interchangeable pathways. In simulation mode, an MCP interface implemented through FastMCP exposes device operations as standardized tool calls. In real-device mode, protocol-specific adapters (MQTT, HTTP) provide the same SmartDevice interface. The RealDeviceAdapter base class extends SmartDevice, ensuring that everything above the Device Layer MCP, agents, blockchain is completely unaware of whether a device is simulated or real. Agents issue *tool calls* downward and receive *results* upward, enabling identical agent logic across simulated and physical devices.

4) Device & Data Layer

The Device & Data layer comprises two subsystems that operate in parallel. The Smart Home Devices subsystem manages IoT devices through three capabilities: Device Types, which define operational characteristics and telemetry schemas; Firmware Safety Bypass, which implements hardware-level emergency overrides that bypass AI entirely through direct actuation; and Telemetry Generation, which produces continuous sensor data streams. The Blockchain & Storage subsystem provides the trust infrastructure through four components: Adaptive PoW Consensus dynamically adjusting mining difficulty, Cryptographic Signing using Ed25519 for every agent transaction, Off-Chain Store maintaining a SQLite database with 13 tables for high-volume data, and Merkle Anchoring computing Merkle roots over off-chain batches and committing them on-chain for tamper detection.

B. SYSTEM ARCHITECTURE (SA) FOR S5-SHB-AGENT

Fig. 3 presents the SA instantiating the RA into deployable components across four layers: Control Plane, Agent Intelligence, Device & Data, and External. The External layer makes explicit the system's dependencies on LLM providers,

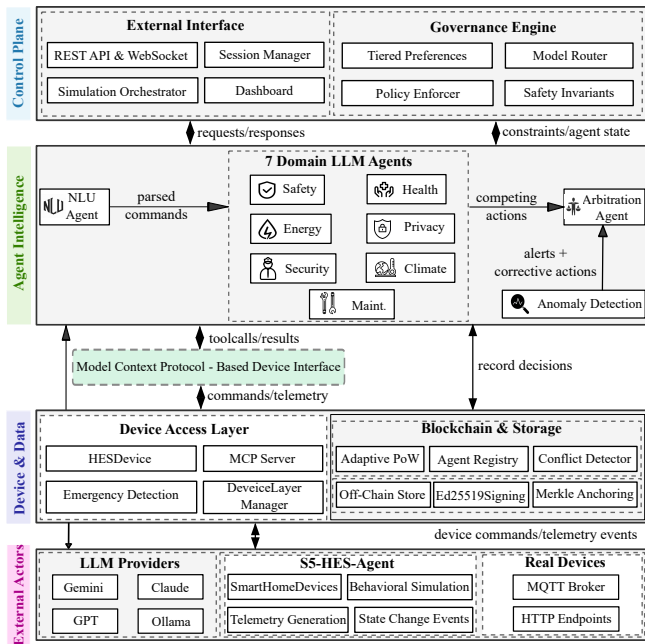


FIGURE 3: System architecture of S5-SHB Agent showing the four-layer implementation with Control Plane, Agent Intelligence, Device & Data, and External layers.

the S5-HES-Agent simulation engine [28], and real device infrastructure.

The Control Plane retains its RA structure with the External Interface (REST API and WebSocket endpoints, Session Manager, Simulation Orchestrator, and Dashboard) and the Governance Engine (Tiered Preferences, Model Router, Governance Contract, and Safety Invariants). The implementation comprises a FastAPI backend on port 8001 with five WebSocket streams for real-time telemetry, blockchain events, agent decisions, governance changes, and scenario state, alongside a Vue.js/TypeScript frontend.

The Agent Intelligence layer implements the 7 Domain LLM Agents (Safety, Health, Security, Privacy, Energy, Climate, Maintenance), NLU Agent, Arbitration Agent, and Anomaly Detection as described in the RA. The MCP Protocol-Based Device Interface mediates between agent tool calls and device commands.

The Device & Data layer contains two subsystems. The Device Access Layer comprises: HESDevice, a universal device class dynamically handling all 118+ device types from S5-HES-Agent; MCP Server providing the FastMCP tool interface with nine tools (device listing, status queries, telemetry collection, command execution, emergency scanning, fallback rules, health checks, fault injection, and device registration); Emergency Scanner implementing reading-based emergency detection that evaluates smoke level and gas concentration thresholds to trigger immediate responses bypassing AI and blockchain; and DeviceLayer Manager coordinating device lifecycle and emergency response. The Blockchain & Storage subsystem comprises six components: Adaptive PoW

for runtime difficulty adjustment, Agent Registry maintaining agent-to-public-key mappings, Conflict Detector identifying competing commands targeting the same device, Off-Chain Store persisting data across 13 SQLite tables, Ed25519 Signing providing per-transaction cryptographic signatures, and Merkle Anchoring bridging off-chain records to on-chain integrity commitments.

The External layer comprises three subsystems. LLM Providers (Google Gemini, Anthropic Claude, OpenAI GPT, and local Ollama) supply reasoning capability through the Model Router. S5-HES-Agent (port 8000) serves as the sole device data source providing device definitions, behavioral simulation, and telemetry generation; S5-SHB Agent consumes all telemetry from S5-HES-Agent through periodic event synchronization. Real Devices connect through MQTT Broker and HTTP Endpoints in real and hybrid deployment modes.

The Simulation Orchestrator coordinates the operational loop: telemetry collection every 10 seconds, off-chain storage, agent reasoning cycles every 20 seconds where each Domain LLM Agent independently analyzes telemetry and proposes actions, conflict resolution through the Arbitration Agent, blockchain mining, and Merkle root anchoring. This cycle operates identically across all deployment modes, with only the telemetry source varying between S5-HES-Agent simulation and physical IoT hardware via protocol adapters. Fig. 4, Fig. 5, and Fig. 6 present the system dashboard interfaces demonstrating the Control Plane implementation—the Simulation View for real-time scenario monitoring, the Blockchain Explorer for inspecting the immutable transaction ledger and chain integrity, and the Agent Monitor for observing multi-agent reasoning cycles and decision outcomes. Together, these interfaces provide the transparent oversight required by Society 5.0 principles.

C. SOLUTION TO DEFINITION 1: ADAPTIVE CONSENSUS BLOCKCHAIN

Definition 1 established that fixed consensus protocols impose static difficulty regardless of workload dynamics, where safety-critical emergency commands require rapid confirmation latency. We address this through the Device & Data layer's Adaptive PoW component implementing runtime difficulty adjustment.

The blockchain maintains a custom lightweight chain where each block B_t contains agent transactions $\{tx_1, tx_2, \dots, tx_k\}$, a SHA-256 hash linking to the previous block, per-transaction SHA-256 hashes, a nonce satisfying the current difficulty target, and a timestamp. The adaptive difficulty mechanism implements Equation (2) through a sliding window estimator.

Let $W = \{B_{t-w+1}, \dots, B_t\}$ denote a sliding window of the w most recent blocks (default $w = 3$). The volume estimator computes:

$$\bar{V}(t) = \frac{1}{|W|} \sum_{B_i \in W} |B_i| \quad (8)$$

where $|B_i|$ denotes the transaction count of block B_i . The dif-

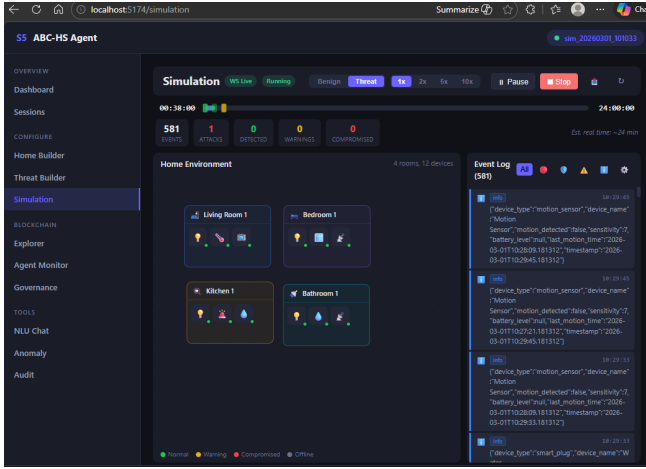


FIGURE 4: Simulation View interface showing real-time threat scenario execution with home environment visualization and live event log streaming.

faculty adjustment follows a stepwise controller with integer increments, clamped within operational bounds:

$$\delta(t+1) = \text{clamp} \left(\begin{cases} \delta(t) - 1, & \text{if } \bar{V}(t) \geq v_{\text{high}} \\ \delta(t) + 1, & \text{if } \bar{V}(t) \leq v_{\text{low}}, \\ \delta_{\min}, \delta_{\max} & \\ \delta(t) \mp 1 \rightarrow \delta_{\text{base}}, & \text{otherwise} \end{cases} \right) \quad (9)$$

where $v_{\text{high}} = 10$ and $v_{\text{low}} = 3$ are volume thresholds, $\delta_{\text{base}} = 2$ is the base difficulty, and $\text{clamp}(\cdot)$ constrains difficulty within $[\delta_{\min}, \delta_{\max}] = [1, 4]$. When average volume falls between thresholds, difficulty gravitates toward δ_{base} through stepwise ± 1 adjustments. High-volume periods including emergencies generating many safety transactions organically lower difficulty for faster mining, while idle periods raise difficulty to conserve resources.

Emergency conditions are handled through the volume-based mechanism rather than an explicit emergency flag. When the Emergency Scanner detects hazardous readings from smoke sensors (threshold ≥ 0.3) or gas detectors ($\text{CO} \geq 50$ ppm, $\text{CO}_2 \geq 5000$ ppm, $\text{NG} \geq 1000$ ppm), the resulting burst of emergency transactions pushes $\bar{V}(t)$ above v_{high} , triggering difficulty reduction. The Emergency Scanner operates at the Device & Data layer, meaning safety response occurs *before* any AI agent reasoning a deliberate design ensuring safety is never bottlenecked by LLM inference time.

Every transaction tx_i carries an Ed25519 digital signature: $\text{sig}(tx_i) = \text{Sign}_{sk_{a_i}}(H(tx_i))$, where sk_{a_i} is the private key of agent a_i and $H(\cdot)$ is SHA-256. The Agent Registry maintains agent-to-public-key mappings, and each transaction passes a four-gate validation pipeline: registration check, signature verification, permission check, and conflict detection. All agents hold wildcard device access at the permission level, enabling unrestricted cross-domain action when safety demands it. Role-based behavioral scoping is enforced through each agent's domain-specific LLM system prompt the Safety

TABLE 3: Agent Specification with Priority

Agent A_i	Responsibility	Priority π	Output Domain
Safety Agent	Fire, gas, smoke response	Safety Critical (1.0)	Emergency commands
Arbitration Agent	Conflict resolution	Safety Critical (0.95)	Resolution decisions
Health Agent	Occupant wellness monitoring	High (0.9)	Health alerts
Anomaly Agent	ML-based anomaly detection	High (0.88)	Anomaly alerts
NLU Agent	Natural language parsing	High (0.85)	Structured commands
Security Agent	Intrusion detection	Medium (0.8)	Lock/alarm actions
Privacy Agent	Camera management	Medium (0.7)	Privacy controls
Energy Agent	Power optimization	Standard (0.6)	Load scheduling
Climate Agent	Temperature, humidity	Standard (0.5)	HVAC commands
Maintenance Agent	Device health monitoring	Standard (0.4)	Maintenance alerts

Agent's prompt focuses on smoke sensors, gas detectors, locks, lights, and thermostats, while the Privacy Agent's prompt directs attention to cameras and smart lights. This ensures no permission constraint can block a safety-critical cross-domain response, while prompt engineering maintains disciplined role separation during normal operation. The complete chain persists to JSON with integrity verification, enabling full audit trail reconstruction.

D. SOLUTION TO DEFINITION 2: MULTI-AGENT DECISION ORCHESTRATION

Definition 2 established that smart home environments require simultaneous reasoning across competing objectives that single-model AI cannot adequately address. We address this through the Agent Intelligence layer's Domain LLM Agents implementing 10 specialized agents with continuous priority values, as formalized in Equation (3) of Section III.

Table 3 presents the complete agent specifications. The priority function $\pi : \mathcal{A} \rightarrow [0, 1]$ assigns each agent a continuous value where higher values indicate greater authority in conflict resolution.

Each Domain LLM Agent a_i operates through a standardized reasoning pipeline. Upon receiving the current telemetry vector $\mathcal{T}(t)$ via the device access interface, the agent constructs a prompt combining its role-specific system prompt σ_i with current device state. The agent dynamically builds a device inventory from actual telemetry readings rather than a hardcoded list, ensuring the prompt always reflects live device states. The LLM returns a structured JSON action command:

$$a_i(\mathcal{T}(t)) = \text{LLM}_i(\sigma_i \parallel \mathcal{T}(t) \parallel \mathcal{G}_{\text{constraints}}) \rightarrow (\text{cmd}_i, \text{conf}_i) \quad (10)$$

where \parallel denotes prompt concatenation, $\mathcal{G}_{\text{constraints}}$ represents governance constraints from the Control Plane, cmd_i is the structured command, and $\text{conf}_i \in [0, 1]$ is the confidence

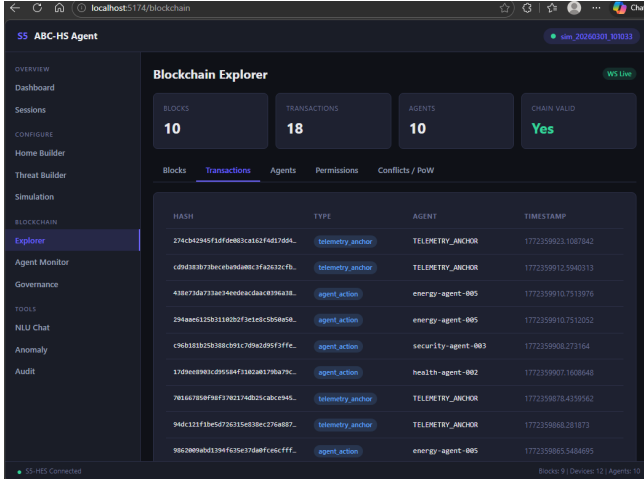


FIGURE 5: Blockchain Explorer interface displaying the immutable transaction ledger with Ed25519-signed transactions, registered agents, and chain validity verification.

score. Governance constraints ensure agents respect resident preferences for example, the Climate Agent cannot set temperature outside the resident’s Tier 1 preferred range.

The reasoning cycle operates every 20 seconds. All Domain LLM Agents execute in parallel via asynchronous concurrent invocation, independently analyzing the same telemetry snapshot. After each agent produces output, the command is SHA-256 hashed, Ed25519 signed, and submitted to the blockchain, producing a tamper-evident audit trail.

Agents operating outside the LLM pipeline provide complementary capabilities. The Anomaly Agent uses a four-model ML/DL ensemble: Isolation Forest, LOF, Z-score, and an optional PyTorch autoencoder. The ensemble flags an anomaly when two or more detectors agree, or when the Isolation Forest score exceeds a critical threshold. Corrective actions are determined through device-specific mappings with a generic fallback for unknown device types. These alerts route to the Arbitration Agent, ensuring anomaly responses pass through the conflict resolution cascade. The NLU Agent parses natural language commands, dynamically building a device catalog from live telemetry and inferring available commands from device readings (e.g., an `is_locked` reading implies lock/unlock). It supports conversation context maintenance and pronoun resolution, translating voice and text inputs into blockchain-signed commands.

Device-level fallback rules ensure continued operation when LLM providers are unavailable. The DeviceLayer Manager maintains reading-based deterministic safety rules automatically adjusting temperature to safe levels when readings exceed 30°C or fall below 16°C executing independently of any AI agent. Additionally, the Emergency Scanner operates at the firmware level for smoke and gas detection without requiring AI or blockchain. This guarantees functional safety even during complete LLM outage.

E. SOLUTION TO DEFINITION 3: MULTI-MODEL LLM ROUTING

Definition 3 established that different agent responsibilities demand different AI capability levels. We address this through the Control Plane’s Model Router implementing tier-constrained multi-provider routing as formalized in Equation (4) of Section III.

The Model Router maintains a provider registry supporting four LLM providers: Google Gemini (primary cloud), Anthropic Claude (secondary cloud), OpenAI GPT (tertiary cloud), and local Ollama (offline inference). Each model is classified into capability tiers $\tau \in \{pro, flash\}$, where “pro” denotes high-capability models for safety-critical reasoning and “flash” denotes cost-efficient models for routine monitoring, with an additional privacy classification $\rho \in \{cloud, local\}$.

The routing function enforces tier constraints:

$$\mathcal{R}(a_i) = \text{select } m_j, \quad \text{s.t. } \tau_j \geq \tau_{\min}(a_i) \quad (11)$$

where τ_{\min} maps agents to minimum model requirements: safety-critical agents (Safety, Health) require “pro” tier; all other LLM-using agents accept “flash” or above; the Anomaly Agent uses ML models, bypassing tier constraints. This constraint is enforced computationally the Model Router rejects any assignment routing a safety-critical agent to a sub-“pro” model regardless of cost pressures.

Per-agent cost tracking accumulates token usage across reasoning cycles:

$$C_{\text{total}}(a_i) = \sum_{t=1}^T C_{\text{token}}(m_{j(t)}) \cdot (|prompt_t| + |response_t|) \quad (12)$$

where $m_{j(t)}$ is the provider assigned at cycle t , C_{token} is the per-token cost, and $|prompt_t|$ and $|response_t|$ are token counts. This enables residents to monitor API expenditure and set budget caps through Tier 3 governance preferences.

The Model Router supports four governance presets *balanced* (pro for safety, flash for others), *max_privacy* (all local Ollama), *budget* (cheapest models with pro for safety), and *best_quality* (pro everywhere) enabling profile switching through governance preference changes. When a provider becomes unavailable, the agent’s deterministic device-level fallback rules activate, ensuring safety responses never depend on potentially unreliable external services.

F. SOLUTION TO DEFINITION 4: INTELLIGENT CONFLICT RESOLUTION

Definition 4 established that multiple agents reasoning over shared device state produce conflicting commands. We address this through the Arbitration Agent implementing the four-level cascade formalized in Equation (5).

Conflict detection operates over pending transactions. When agents a_i and a_j submit commands targeting the same device d_k with different actions, the Conflict Detector flags a conflict. Let $\mathcal{F}_{\text{conflict}} = \{(cmd_i, cmd_j, d_k) : device(cmd_i) =$

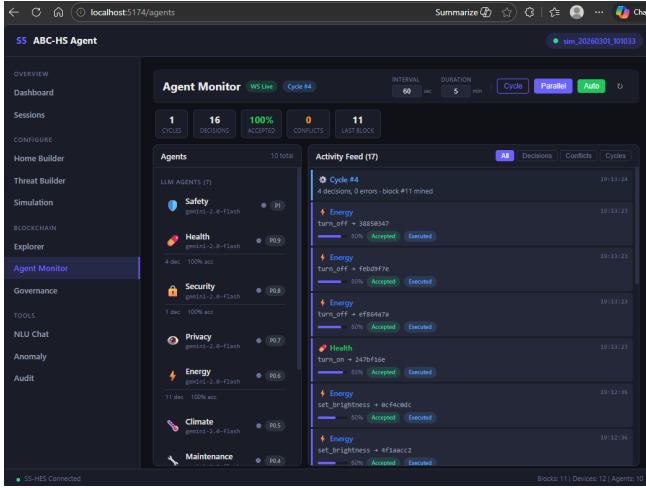


FIGURE 6: Agent Monitor interface showing multi-agent reasoning cycles with per-agent decisions, confidence scores, and real-time activity feed.

$device(cmd_j) = d_k, action(cmd_i) \neq action(cmd_j)$ denote the detected conflict set.

L1: Safety Override. If either command originates from the Safety Agent (a_s with $\pi = 1.0$), it wins unconditionally:

$$\mathcal{CR}_{L1}(cmd_i, cmd_j) = cmd_s, \quad \text{if } a_s = \text{safety-agent-001} \quad (13)$$

This override is an *immutable invariant* it cannot be modified by governance, agent reasoning, or external input. The Safety Agent’s authority is architecturally enforced, not merely a software policy.

L2: LLM Arbitration. For non-safety conflicts, the Arbitration Agent invokes an LLM to analyze full situational context:

$$cmd_{winner} = \mathcal{L}(cmd_i, cmd_j, \mathcal{T}(t), \mathcal{G}_{prefs}, \pi) \quad (14)$$

where $\mathcal{T}(t)$ is current telemetry, \mathcal{G}_{prefs} represents resident governance preferences, and π provides priority values and historical scores. The LLM selects the command best satisfying preferences while respecting governance constraints.

L3: ML Scoring. If LLM arbitration fails, historical agent performance scoring activates:

$$\mathcal{S}(a_i) = 0.6 \cdot \underbrace{r_{accept}(a_i) \cdot (1 - 0.5 \cdot r_{conflict}(a_i))}_{\text{ML historical score}} + 0.4 \cdot \pi(a_i) \quad (15)$$

where $r_{accept}(a_i)$ is the acceptance rate, $r_{conflict}(a_i)$ is the conflict rate, and $\pi(a_i)$ is priority. The ML component (60%) captures learned patterns; priority (40%) provides a stable baseline. The highest composite score wins.

L4: Priority Fallback. As the deterministic backstop:

$$cmd_{winner} = cmd_{\arg \max_{a_i} \pi(a_i)} \quad (16)$$

ensuring resolution even under complete LLM and ML failure. Every conflict record including commands, resolution level, winner rationale, and outcome is logged to off-chain

TABLE 4: Four-Tiered Governance Preference Hierarchy

Tier	Scope	Parameters (Count)	Mutability
G_1 (Safe)	Routine adjustments	Temperature, brightness, quiet hours, voice, alerts (8 keys)	Resident-modifiable
G_2 (Impactful)	Trade-off settings	Comfort-vs-energy, security-vs-privacy, automation level (7 keys)	Resident-modifiable with validation
G_3 (Advanced)	System overrides	Per-agent device overrides, API budget caps, allowed providers (3 keys)	Resident-modifiable with validation
G_4 (Locked)	Safety invariants	Safety thresholds, crypto settings, override authority (9 keys)	Immutable

storage and anchored on-chain, producing a complete auditable history of inter-agent disputes.

G. SOLUTION TO DEFINITION 5: HUMAN-CENTERED TIERED GOVERNANCE

Definition 5 established that Society 5.0 principles demand residents retain meaningful control while being shielded from multi-agent AI complexity. We address this through the Governance Engine implementing the four-tier preference model formalized in Equation (6).

The Governance Contract manages the hierarchy $\mathcal{G} = \{G_1, G_2, G_3, G_4\}$ where each tier encompasses defined resident influence with monotonically increasing impact and stricter validation. Table 4 presents the tier specification.

The authorization function from Equation (6) is implemented as a validation pipeline:

$$\phi(\mathcal{P}_u, G_k) = \begin{cases} allow, & \text{if } k \leq 3 \text{ and } \text{valid}(v, R_k) \\ deny, & \text{if } k = 4 \quad \forall u \end{cases} \quad (17)$$

where $\text{valid}(v, R_k)$ checks the proposed value against 12 typed validation rules (range bounds for numerical parameters, choice sets for categorical parameters, type constraints). Tiers 1-3 are resident-accessible with validation ensuring values remain within safe bounds (e.g., temperature $\in [16, 30]^\circ\text{C}$, comfort-vs-energy $\in [0, 1]$, API budget $\in [0, 1000]$). Tier 4 is computationally immutable the Governance Contract rejects any Tier 4 modification regardless of requester identity, enforced at the code level with no override mechanism.

The governance flow integrates with the agent pipeline through the *constraints* channel. When a resident modifies preferences, the Governance Engine propagates updated constraints to all agents. Agents incorporate these via the $\mathcal{G}_{constraints}$ parameter in Equation (10), ensuring subsequent reasoning respects updated preferences. Tier 2 trade-off sliders dynamically adjust agent priority values through calibrated formulas, directly influencing conflict resolution outcomes.

The NLU Agent enables non-technical residents to exercise governance through natural language a resident can say ‘‘I

TABLE 5: Society 5.0 Governance Compliance Dimensions and Three-Level Rubric

Dim	Name	× Absent	√ Partial	√√ Full
D1	Resident Authority	No user-configurable params	Binary permissions (grant/deny)	Graduated multi-tier control
D2	Safety Immutability	No safety protection	General blockchain tamper-resistance	Specific safety params locked at code level
D3	Governance Granularity	Single-level flat governance	2 levels (e.g. owner/user)	3+ graduated tiers with distinct permissions
D4	Audit Completeness	No audit trail	Some transaction logging	All governance mutation types audited
D5	Validation Coverage	No input validation	Identity/permission checks only	Type + bound validation on mutable params
D6	Conflict Resolution	No mechanism	Simple priority-based	Multi-level arbitration cascade

prefer comfort over energy savings” and the NLU Agent translates this into a Tier 2 parameter update. All governance changes regardless of input modality are validated by the Governance Contract and logged as on-chain transactions, producing an audit trail serving the Society 5.0 principle of technology accountability to human oversight.

H. SOLUTION TO DEFINITION 6: MULTI-MODE DEPLOYMENT WITH TAMPER-EVIDENT ANCHORING

Definition 6 established that practical research requires flexible evaluation across simulation, real hardware, and hybrid configurations with verifiable data integrity. Among 21 surveyed works, only [22] and [17] achieve partial hybrid deployment; neither offers user-selectable mode switching. We address this through the Simulation Orchestrator coordinating the operational loop across deployment modes with Merkle-based tamper-evident anchoring.

The framework supports three modes $\mathcal{O} = \{sim, real, hyb\}$ through a unified interface. In simulation mode, the Device & Data layer generates synthetic telemetry accessed through the MCP tool interface. In real mode, protocol-specific adapters `MQTTDeviceAdapter` for MQTT-based devices, `HTTPDeviceAdapter` for REST-based devices connect to physical hardware, extending the same `SmartDevice` base class so the agent and blockchain stack operates identically. In hybrid mode, devices are independently routed to real or simulated adapters. An `AdapterRegistry` maps protocol names to adapter classes, allowing new protocols without modifying existing code.

The Simulation Orchestrator implements a deterministic cycle operating identically across modes:

$$\text{Cycle}(t) : \mathcal{T}(t) \xrightarrow{\text{store}} \mathcal{D}_{\text{off}} \xrightarrow{\text{reason}} \{cmd_i\} \xrightarrow{\text{resolve}} cmd^* \xrightarrow{\text{mine}} B_t \quad (18)$$

where telemetry $\mathcal{T}(t)$ is collected every 10 seconds, stored in the off-chain SQLite database \mathcal{D}_{off} (13 tables: continuous telemetry, event telemetry, alerts, reasoning logs, telemetry anchors, conflict records, decision outcomes, MCP health, NLU conversations, anomaly logs, arbitration logs, governance changes, and model usage), processed by agents every 20 seconds to produce commands $\{cmd_i\}$, resolved through the cascade to produce cmd^* , and mined into block B_t .

Tamper-evident anchoring uses Merkle trees to bridge off-chain storage with on-chain integrity. At configurable intervals, recent off-chain records are batched and a Merkle root

computed:

$$\mathcal{M}_r = \text{MerkleRoot}(\{H(rec_1), H(rec_2), \dots, H(rec_n)\}) \quad (19)$$

where $H(\cdot)$ is SHA-256 and $\{rec_i\}$ are off-chain records generated since the last anchoring event. The Merkle root \mathcal{M}_r is committed on-chain as an anchoring transaction, enabling efficient tamper detection: any modification to an off-chain record invalidates the Merkle proof path verifiable against the on-chain commitment. This allows high-frequency telemetry to be stored efficiently off-chain while maintaining blockchain-grade integrity through periodic Merkle commitments.

The complete deployment function satisfies Definition 6:

$$\mathcal{S}_{\text{deploy}}(\omega, \mathcal{D}_{\text{off}}) = (\mathcal{B}_{\text{chain}}, \mathcal{M}_r), \quad \omega \in \mathcal{O} \quad (20)$$

producing blockchain-anchored records $\mathcal{B}_{\text{chain}}$ with Merkle root commitments \mathcal{M}_r regardless of deployment mode ω . Five WebSocket streams (telemetry, blockchain, agents, governance, scenarios) provide real-time observability across all modes, enabling transparent monitoring by researchers and residents alike. This multi-mode capability addresses the deployment flexibility gap identified across all 21 surveyed works.

V. EVALUATION

In this section, we present the evaluation of the S5-SHB Agent. Section V-A describes the evaluation metrics. Section V-B presents the experiment setup. We present evaluation results in Section V-C, V-D, V-E and V-F. Discussion is conducted in Section V-F.

A. EVALUATION METRICS

We prepare the evaluation matrix under four pillars based on four key questions as follows.

- Governance model validation aims to evaluate;
 - Existing systems’ Society 5.0 governance requirements across six dimensions shown in Table 5.
 - Resident governance sliders’ impact on agents’ priorities.
 - Security and privacy variances with respect to agents’ responses to resident inputs.
- Blockchain performance investigates;
 - Mining latency under each operational phase for static and adaptive difficulty configurations.
 - Computational overhead (time, hash iterations, throughput) that adaptive difficulty imposes over a full run.

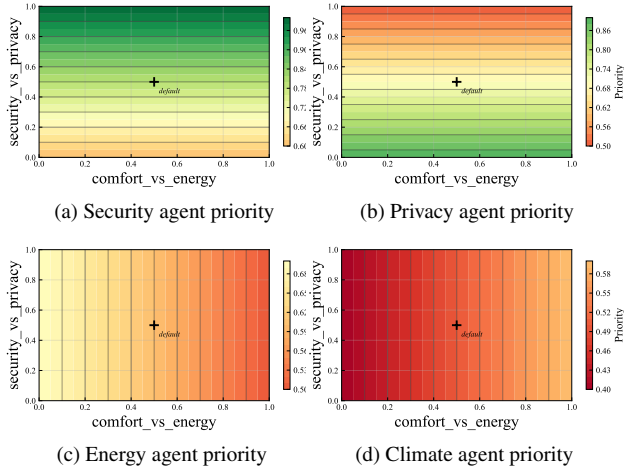


FIGURE 7: Agent priority contour surfaces over the 21×21 governance slider grid. Each subplot shows one adjustable agent’s priority as a function of *comfort_vs_energy* (horizontal) and *security_vs_privacy* (vertical).

- Difficulty adjustment behavior of each adaptive profile across phase transitions.
- Compare our measured latency, throughput, memory, and emergency response against literature-reported IoT blockchain platforms.
- Multi-Agent system;
 - Measure decision confidence and agent activation patterns across four Gemini model variants under baseline and threat conditions.
 - Quantify how each model’s transaction generation rate affects blockchain throughput and adaptive difficulty behavior.
- System validation
 - Verify that the PoW mining effort remains computationally bounded
 - Confirm that all agent decisions are accepted and that confidence remains stable when threats are present.
 - Profile the real-world latency of each agent role and the blockchain’s transaction packing density to establish deployment bounds.

B. EXPERIMENTAL SETUP

All experiments were conducted on a single workstation equipped with an AMD Ryzen AI 9 HX 370 processor (24 CPUs, 2.0 GHz base clock) with Radeon 890M integrated graphics, running Windows 11 with Python 3.13.5. The evaluation is organized into three independent pillars and one integrative system validation layer. Pillar 1 (Governance) is fully deterministic and requires no external API calls, validating the four-tier governance model across six compliance dimensions and a 21×21 slider sweep of 441 configurations. Pillar 2 (Blockchain) evaluates five configurations (two static Proof-of-Work baselines and three adaptive variants) over ten

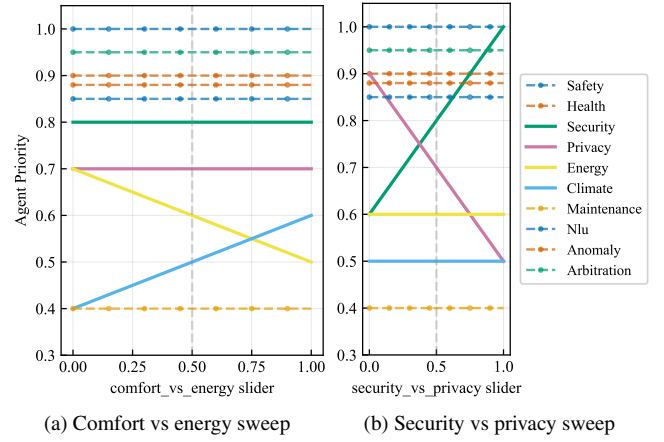


FIGURE 8: Priority trajectories of all ten agents along each governance slider axis. Invariant agents (dashed) maintain fixed priorities; adjustable agents (solid) respond to slider changes.

independent runs each, using a four-phase workload of 20 blocks and 108 transactions shared across all experiments. Pillar 3 (Multi-Agent) and System Validation require live API calls through the Google Gemini API; Pillar 3 executes eight sessions (four Gemini model variants across two conditions: baseline and threat-injected), each comprising 30 cycles over 16 simulated devices, while System Validation runs ten sessions (five baseline and five threat) using gemini-2.0-flash to exercise the complete telemetry-to-blockchain pipeline. A fixed random seed (SEED = 42) is applied throughout all stochastic experiments. Quantitative claims are accompanied by 95% confidence intervals computed via the t-distribution (ddof = 1). Multi-group comparisons use the Kruskal-Wallis H test, followed by pairwise Mann-Whitney U tests with Bonferroni correction; effect sizes are reported as Cohen’s d, and Shapiro-Wilk tests verify distributional assumptions.

C. GOVERNANCE MODEL VALIDATION

To evaluate the governance model, we conducted three main experiments as mentioned in Section V-A. Table 6 evaluates whether existing systems satisfy Society 5.0 governance requirements across six dimensions. We define six governance dimensions (D1-D6) derived from Society 5.0 principles and classify each system as *Absent*, *Partial*, or *Full* per dimension based on verifiable evidence from the original publications.

TABLE 6: Governance Feature-Presence Comparison

Dimension	Ours	[4]	[15]	[16]	[19]	[20]
D1 Resident Authority	✓✓	✓	✓	✓	×	×
D2 Safety Immutability	✓✓	✓	✓	✓	✓	✓✓
D3 Governance Granularity	✓✓	✓	✓	✓	✓	×
D4 Audit Completeness	✓✓	✓	✓	✓	✓	✓
D5 Validation Coverage	✓	✓	✓	✓	✓	✓
D6 Conflict Resolution	✓✓	×	×	×	×	×

✓✓ Full ✓ Partial × Absent

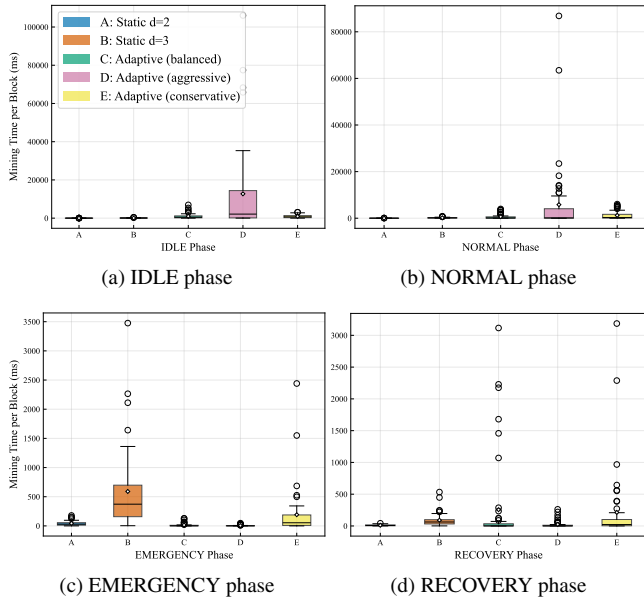


FIGURE 9: Per-block mining time distribution across five configurations (A-E) for each operational phase. Adaptive configurations reduce difficulty during EMERGENCY, yielding sub-15 ms block commits compared to 590 ms for static $d=3$.

Our system and five related works are compared side by side. Fig. 7 evaluates whether resident governance sliders produce a continuous and bounded effect on agent priorities. Both governance sliders (*comfort-vs-energy* and *security-vs-privacy*) are swept from 0 to 1 in 0.05 increments, forming a 21×21 grid of 441 configurations. For each configuration, the four adjustable agent priorities are computed deterministically and plotted as filled contour surfaces. In Fig. 8, we evaluate whether safety-critical agents remain invariant while adjustable agents respond to resident input. One slider is swept from 0 to 1 while the other is held at the default (0.5), and all ten agent priorities are plotted as lines. Invariant agents appear as flat horizontal lines; adjustable agents appear as sloped lines.

Our system achieves *Full* on five of six dimensions (D1-D4, D6), with only D5 (Validation Coverage) at *Partial* - 12 of 18 mutable parameters currently have type and bound validation rules. None of the five related works achieves *Full* in more than one dimension: [20] reaches *Full* on D2 via firmware hash verification via its COTA smart contract, whereas [4], [15], and [16] remain at *Partial* across all dimensions. [19] and [20] score *Absent* on D1 (Resident Authority) because their architectures are entirely system-managed with no resident-configurable governance parameters. The most distinguishing result is D6 (Conflict Resolution), where all five related works score *Absent*, none implements any mechanism for resolving competing governance objectives, while our system provides a four-level arbitration cascade (safety override, LLM reasoning, ML prediction, priority fallback).

The Security and Privacy subplots show horizontal con-

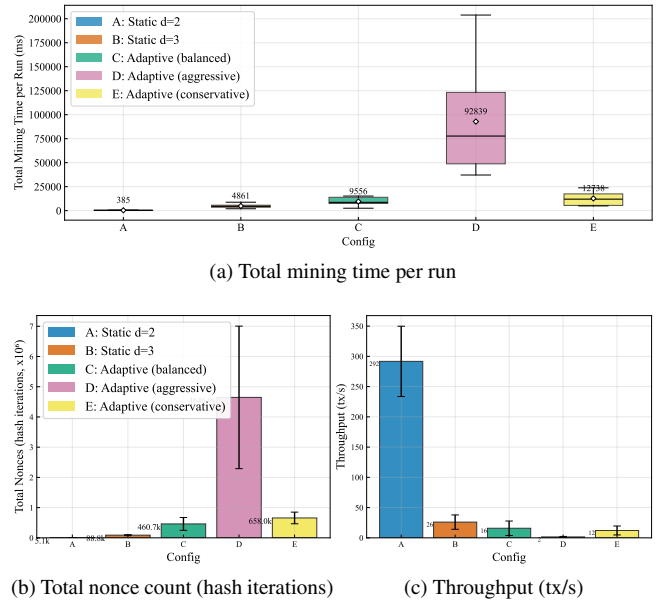


FIGURE 10: Computing cost of mining across five configurations. (a) End-to-end mining time for a 108-txn run. (b) Total hash iterations required. (c) Resulting txn throughput. Config C (balanced) achieves a practical trade-off at 9.6 s and 16 tx/s, while Config D (aggressive) consumes 93 s for only 2 tx/s.

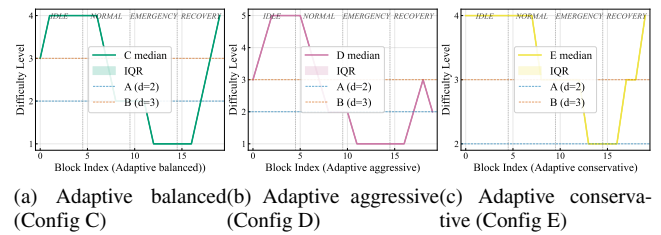


FIGURE 11: Block-by-block difficulty traces across the four operational phases (IDLE, NORMAL, EMERGENCY, RECOVERY). Solid lines show median difficulty over 10 runs; shaded bands show IQR. Dashed lines mark static baselines A ($d=2$) and B ($d=3$). Config C adapts smoothly with a 2-block lag, Config D overshoots to $d=5$ and oscillates in RECOVERY, and Config E stays within $[2, 4]$ and under-reacts during EMERGENCY.

tour bands; their priorities depend solely on the security-vs-privacy slider and are unaffected by comfort-vs-energy. Conversely, Energy and Climate produce vertical bands tied only to comfort-vs-energy. This confirms that the two slider axes govern orthogonal agent pairs with no cross-coupling. Security spans the widest range $[0.6, 1.0]$, reaching parity with the Safety agent at the extreme, while Climate occupies the narrowest band $[0.4, 0.6]$. The default configuration (0.5, 0.5), indicated in each subplot, recovers the baseline priority values exactly, so the governance layer introduces no behavioural change when the resident has not expressed a preference.

TABLE 7: Our measured blockchain performance across five configurations.

Config	Type	Latency (ms/blk)	Throughput (tx/s)	Memory (KB)	Storage (KB)	Emergency (ms)
A	Static d=2	19.3	291.7	61.9	55.1	43.3
B	Static d=3	243.1	26.0	61.9	55.1	590.2
C	Adaptive (balanced)	477.8	15.9	61.7	55.1	15.2
D	Adaptive (aggressive)	4641.9	1.5	61.7	55.1	5.4
E	Adaptive (conservative)	636.9	12.2	61.8	55.1	191.7

TABLE 8: Literature-reported blockchain latency.

Platform	Latency (ms)
OmniBlock PoW [20]	2713.7
OmniBlock Raft [20]	1102.6
Xia HLF [21]	850.0
Erukala HLF [8]	590.0
Arshad HLF [22]	570.0
Arshad Eth-PoA [22]	360.0
Arshad Algorand [22]	310.0
Arshad IOTA [22]	220.0

TABLE 9: Literature-reported blockchain throughput.

Platform	Throughput (tx/s)
Arshad Algorand [22]	910
Xia HLF [21]	658
Arshad Eth-PoA [22]	620
Arshad IOTA [22]	560
Arshad HLF [22]	410
Erukala HLF [8]	122

Six of ten agents, Safety (1.00), Arbitration (0.95), Health (0.90), Anomaly (0.88), NLU (0.85), and Maintenance (0.40) hold perfectly flat lines across both sweeps, confirming that no slider combination can alter their behaviour. The remaining four trace linear slopes: in Fig. 7a, Energy falls from 0.7 to 0.5, and Climate rises from 0.4 to 0.6 as comfort-vs-energy increases, while Security and Privacy stay flat at their default values. Fig. 7b mirrors this. Security climbs from 0.6 to 1.0, and Privacy drops from 0.9 to 0.5 along the security-vs-privacy axis, with Energy and Climate unchanged. Crucially, Safety and Arbitration remain above all adjustable agents at all slider positions, ensuring that the priority hierarchy protecting residents from unsafe outcomes is never violated.

D. BLOCKCHAIN PERFORMANCE

All four experiments share a common workload and configuration set. Five blockchain configurations are tested: two static baselines (A: fixed d=2, B: fixed d=3) and three adaptive profiles (C: balanced, D: aggressive, E: conservative) that differ in window size, difficulty range, and transition thresholds. Each configuration runs 10 independent times (seed=42) over a 20-block workload divided into four phases, IDLE (5 blocks, 1-2 tx), NORMAL (5 blocks, 4-6 tx), EMERGENCY (5 blocks, 10-15 tx), and RECOVERY (5 blocks, 2-3 tx) - totalling 108 transactions per run. Per-block mining time is measured in seconds, and the PoW solver records nonce counts. All experiments draw from the same cached raw dataset (1000 rows = 5 configs x 10 runs x 20 blocks).

For Fig. 9, the raw per-block mining times are grouped by phase and configuration, then plotted as box plots, one subplot per phase. This isolates how each configuration behaves under different transaction loads, making the emergency-

phase latency drop directly visible.

In Fig. 10, per-run totals are aggregated from the same raw data: total mining time is the sum of all 20 block times, total nonces is the sum of all hash iterations, and throughput is 108 transactions divided by total mining time in seconds. The three bar charts present these as complementary views of the same computational cost.

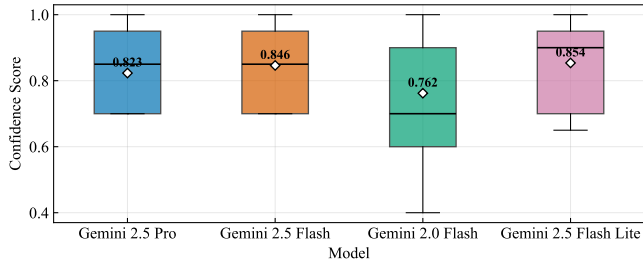
Fig. 11 evaluates each adaptive configuration (C, D, E), and the difficulty level at each block index is extracted across all 10 runs. The median difficulty is plotted as a solid line with IQR shading, overlaid on the static baselines A and B as dashed reference lines. Phase boundaries are marked as vertical separators.

Table 7 summarises our five configurations on latency, throughput, memory, storage, and emergency response all derived from Experiments. Table 8 collects literature-reported values from six referenced works covering Hyperledger Fabric, Ethereum-PoA, IOTA, Algorand, and OmniBlock, cited as reported by the original authors.

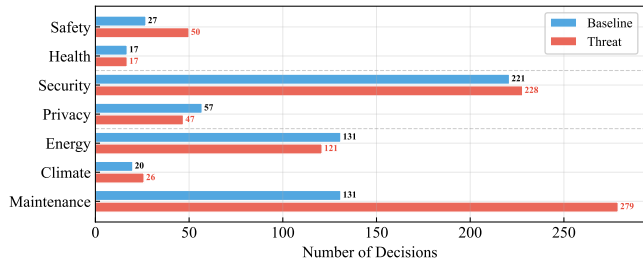
Fig. 9a represents IDLE. Static A and B mines take under 100 ms, whereas adaptive configs increase difficulty during low-activity conditions D inflates. NORMAL phase presented in Fig. 9b. Adaptive configs begin easing off as transaction volume rises; D still shows outliers, but C dropped, indicating the algorithm is already responding.

Fig. 9c is EMERGENCY. The ranking flips: static B stays at 590 ms mean, while C and D drop to 15 ms and 5 ms, respectively, by reducing difficulty to d=1. Fig. 9d represents RECOVERY. All configs return to moderate latencies, though C and E show long-tail outliers (up to 3 s) as the algorithm ramps difficulty back up. Across the four phases, the adaptive mechanism trades higher idle-phase latency for near-instant emergency commits. Static baselines remain consistent but cannot respond to phase changes.

Fig. 10a represents total mining time. Config A completes the entire 108-transaction run in 385 ms mean, while D takes 92,839 ms, a 240x gap. Fig. 10b is the total nonces. The hash iteration counts mirror the timing pattern: A requires 5.1k nonces, B 88.8k, C 460.7k, and D 4,646.9k. D consumes 10x more hashes than C for the same 108 transactions, confirming its d=5 ceiling is disproportionately expensive. Fig. 10c shows Throughput. A achieves 292 tx/s, B drops to 26, C to 16, and D collapses to 2 tx/s. E sits at 12 tx/s, comparable to C despite its narrower difficulty range. Adaptive difficulty costs more than static baselines, but the cost varies enormously with tuning. Config D's aggressive profile pushes difficulty so high during idle periods that its overall overhead dwarfs all other configs 10x more nonces and 10x less throughput than C, for marginal emergency gains (5 ms vs 15 ms). Config C strikes



(a) Confidence distribution per model (baseline)

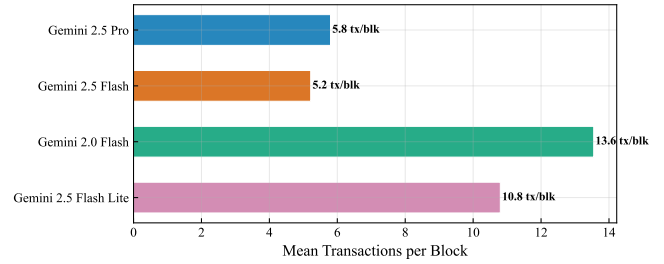


(b) Decision volume per agent role under baseline and threat conditions

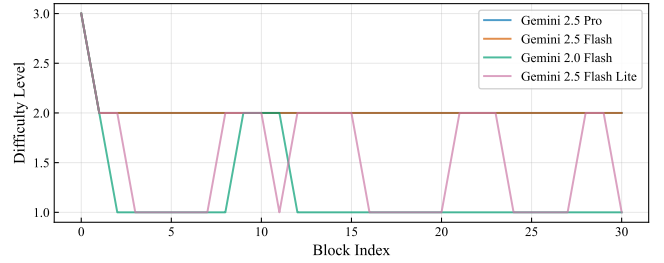
FIGURE 12: Multi-agent decision quality across four Gemini model variants. (a) Box plots of per-decision confidence scores from baseline sessions, with mean values annotated. (b) Number of decisions issued by each agent role, comparing baseline (no faults) against threat (7 injected faults), aggregated across all models.

a practical balance: its 16 tx/s throughput is sufficient for a single household generating tens of transactions per hour, and its 9.6 s total mining time falls within the range of a Raspberry Pi-class device.

Fig.11a is Config C (balanced). Difficulty rises to $d=4$ during IDLE, holds through early NORMAL, then descends smoothly toward $d=2$ as transaction volume increases. At the EMERGENCY boundary it drops to $d=1$ within 2 blocks and stays there, then climbs back through RECOVERY to $d=4$. Fig. 11b represents Config D (aggressive). The trace peaks at $d=5$ during IDLE - one level above C's ceiling - and drops abruptly to $d=1$ at the emergency onset in a single block. During RECOVERY, the line spikes and dips between $d=1$ and $d=3$ before settling, revealing oscillatory behaviour. Fig. 11c shows Config E (conservative). Difficulty holds flat at $d=4$ through IDLE and most of NORMAL, with only a brief dip around the NORMAL midpoint. It drops to $d=2$ during EMERGENCY, does not reach $d=1$ because its floor is clamped at $d=2$, and returns to $d=3-4$ in RECOVERY. The three traces explain the cost and latency differences seen in Experiments 1 and 2. Config D's peak at $d=5$ accounts for its extreme idle-phase mining times; its single-block emergency drop explains its 5 ms latency; its recovery oscillation explains the variance in that phase. Config E's refusal to drop below $d=2$ explains why its emergency latency (192 ms) is an order of magnitude above C and D. Config C's smooth, bounded transitions between $d=1$ and $d=4$ with no oscillation and a 2-block adaptation lag make it the most predictable



(a) Mean transactions per block by model



(b) Adaptive difficulty trace over 30 blocks

FIGURE 13: Blockchain behavior under multi-model agent load. (a) Average number of txns committed per block for each Gemini variant, reflects differences in decision verbosity. (b) Difficulty level at each block index, shows Flash holds a stable $d=2$ while 2.0 Flash and Flash Lite oscillate between $d=1$ and $d=2$ in response to their higher txn rates.

profile while still achieving the full emergency drop.

Table 7 shows our five configurations. All five share the same memory (62 KB) and storage (55 KB) footprints, as these depend on chain length rather than difficulty. Config A has the lowest overall latency (19.3 ms/block) and highest throughput (292 tx/s), but no phase adaptation. Config C offers the best trade-off among adaptive profiles: 478 ms overall latency, 16 tx/s throughput, and 6.8 ms emergency response. Config D achieves the fastest emergency time (3.0 ms) but its 4,642 ms overall latency and 1.5 tx/s throughput rule it out for practical use. Table 8 is a literature comparison. The fastest distributed platform, IOTA, reports a latency of 220 ms with 42 MB of memory. Our Config C matches this latency range overall (478 ms) while using 694x less memory (62 KB vs 42 MB). Where the gap widens in our favour is emergency response: Config C commits blocks in 6.8 ms during emergencies - 32x faster than IOTA's steady-state 220 ms. Throughput is where we concede: 16 tx/s (Config C) compared to 122-910 tx/s in the literature, which is expected given that our blockchain is a single-node edge-layer serving a single household, not a distributed network handling concurrent clients. The two tables together demonstrate that our blockchain is not a general-purpose replacement for distributed platforms. It is a fit-for-purpose edge layer where sub-10 ms emergency commits and a sub-100 KB footprint matter more than raw throughput - and on those two dimensions, no other platform in the literature comes close.

E. MULTI-AGENT SYSTEM

Figure 12 presents the results of all eight sessions (4 models x 2 conditions) run over 30 decision cycles on a 16-device, 4-room simulated household. Threat sessions inject 7 faults at cycles 11-23 (smoke, gas leak, intrusion, temperature spike, motion, power surge, cascading emergency), each persisting for 2 cycles before auto-clearing; baseline sessions run the same 30 cycles with no injections. For subplot (a), per-decision confidence scores from the four baseline sessions are grouped by model and plotted as box plots to isolate model-level reasoning quality without threat interference. For subplot (b), decisions from all eight sessions are split into baseline and threat groups, then counted per agent role across all models combined, producing paired horizontal bars that reveal which agent categories activate more under threat. Fig. 13 shows the same eight sessions provide blockchain records - 240 blocks and 2,122 transactions in total. For subplot (a), the total transactions in each session are divided by its block count to obtain the mean transactions per block, and these are then averaged across baseline and threat conditions for each model and plotted as horizontal bars. For subplot (b), the adaptive difficulty level recorded at each block index is plotted as a line trace for each model across all 30 blocks, showing how the PoW algorithm responds differently to each model's transaction-volume pattern.

Fig. 12a is the confidence distribution. Flash Lite achieves the highest mean confidence (0.854), closely followed by Flash (0.846) and Pro (0.823), while 2.0 Flash trails at 0.762 with the widest interquartile range and whiskers extending down to 0.4. The three 2.5-generation models cluster within a narrow 0.82-0.85 band, whereas 2.0 Flash sits significantly below them (Mann-Whitney $p < 0.001$, medium effect size $d = 0.55-0.64$). Fig. 12b Decision volume. Safety and maintenance agents show the largest threat-driven increases - safety nearly doubles from 27 to 50 decisions (+85%) and maintenance more than doubles from 131 to 279 (+113%), reflecting correct escalation toward fault detection and device recovery. Health remains unchanged at 17 decisions in both conditions, and security stays stable (221 vs 228), indicating that agents not directly targeted by the injected faults maintain their baseline workload rather than generating spurious activity. The two subplots together confirm that the multi-agent system is both model-robust and threat-responsive. All four models produce near-ceiling acceptance rates (99-100%) regardless of variant, so the practical differentiator is confidence calibration - where 2.5-generation models hold a clear advantage. Meanwhile, the shift in decision volume under threat follows a logical pattern: safety-critical and recovery agents scale up while unrelated agents hold steady, demonstrating that the arbitration layer routes threats to the appropriate responders without over-activating the rest of the system.

Fig. 13a presents the throughput. Gemini 2.0 Flash commits 13.6 transactions per block on average - more than double Pro (5.8) and Flash (5.2) - because it produces shorter, more frequent agent outputs that the blockchain batches into denser blocks. Flash Lite sits in between at 10.8 tx/blk, sug-

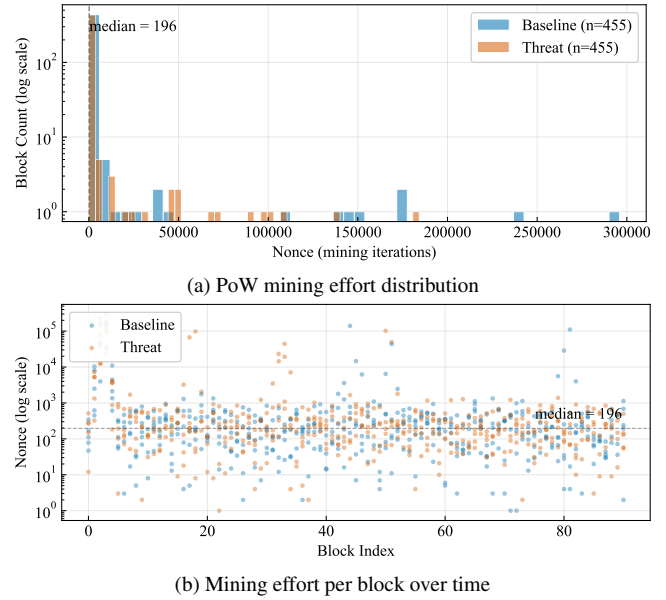


FIGURE 14: Blockchain mining integrity across 910 blocks (5 baseline + 5 threat sessions). (a) Nonce distribution with median of 196 iterations; baseline and threat overlap almost entirely. (b) Per-block nonce over block index showing no temporal drift in either condition.

gesting that lighter models tend to generate higher transaction volumes per decision cycle. Fig. 13b shows the difficulty trace. Flash holds a constant $d=2$ across all 30 blocks, making it the most predictable model from the blockchain's perspective. Pro drops from $d=3$ to $d=1$ within the first two blocks and remains there, reflecting its lower transaction rate. Both 2.0 Flash and Flash Lite oscillate between $d=1$ and $d=2$ throughout the run, with repeated spikes wherever a burst of transactions triggers the adaptive algorithm to briefly raise difficulty before the next low-volume interval pulls it back down. The throughput and difficulty results are directly linked: models that pack more transactions per block create uneven load patterns that force the adaptive PoW to oscillate, whereas models with moderate, steady output allow the difficulty to settle. From a deployment standpoint, Flash is the most blockchain-friendly variant - its stable $d=2$ avoids both the wasted overhead of difficulty spikes and the reduced tamper resistance of prolonged $d=1$ operation.

F. SYSTEM VALIDATION

All three experiments share a common workload: 5 baseline and 5 threat sessions, each running 30 decision cycles on a single model (Gemini 2.0 Flash) across a 16-device, 4-room household. Threat sessions inject 7 faults at cycles 11-23, each persisting for 2 cycles before auto-clearing. Each session produces 91 blocks (910 in total across all runs), and each block records its PoW solver nonce count. For Fig. 14a, nonces from all 910 blocks are split by condition and binned into a 50-bin histogram on a log Y-scale, with the overall

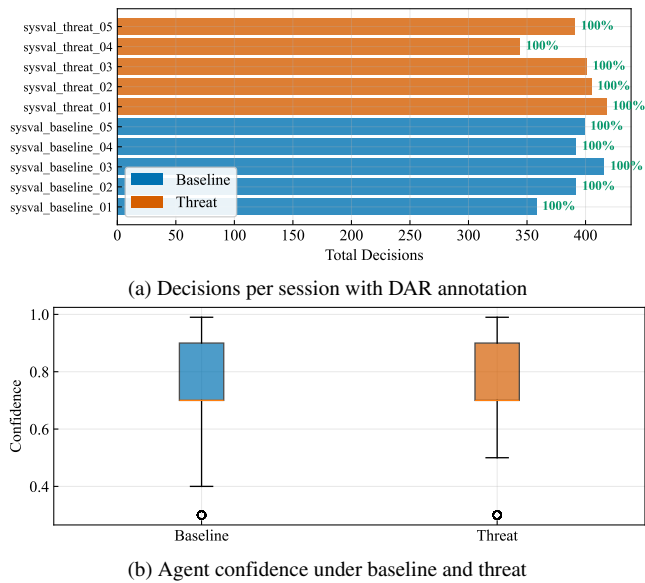


FIGURE 15: Agent decision reliability over 10 repeated sessions. (a) All sessions achieve 100% decision acceptance rate across 3,916 decisions. (b) Confidence distributions share the same median (0.90) under both conditions, confirming that threat injection does not degrade reasoning quality.

median marked as a dashed reference line. For Fig. 14b, each block's nonce is plotted against its block index on a log Y-scale, with baseline and threat points distinguished by colour to check whether mining effort drifts over time.

Fig. 15 presents decision records from all 10 sessions are loaded (3,916 total), where each record carries its session name, acceptance flag, and confidence score. For Fig. 15a, the total accepted decisions per session are plotted as horizontal bars with the DAR percentage annotated beside each bar. For Fig. 15b, all per-decision confidence scores are grouped into baseline and threat pools and displayed as side-by-side box plots to compare reasoning quality across conditions.

Fig. 16 presents the model usage logs (3,733 LLM calls) provide per-call latency and agent identity, while blockchain records provide per-block transaction counts and block type. For Fig. 16a, latencies are grouped by agent role and displayed as horizontal box plots ordered from fastest to slowest median. For Fig. 16b, each block's transaction count is plotted against its block index, with background shading separating anchor blocks (1 tx, Merkle anchors) from decision blocks (5-17 tx, agent transactions).

Fig. 14a shows PoW mining effort distribution. The histogram is sharply right-skewed: the vast majority of blocks resolve within the first bin (under 5,000 nonces), with a median of just 196 iterations, while a sparse tail stretches out to roughly 296,000. Baseline ($n = 455$) and threat ($n = 455$) bars overlap almost entirely across all 50 bins, showing no measurable shift in mining cost when threats are active. Fig. 14b presents mining effort over time. The scatter plot confirms that the distribution in subplot (a) is stationary -

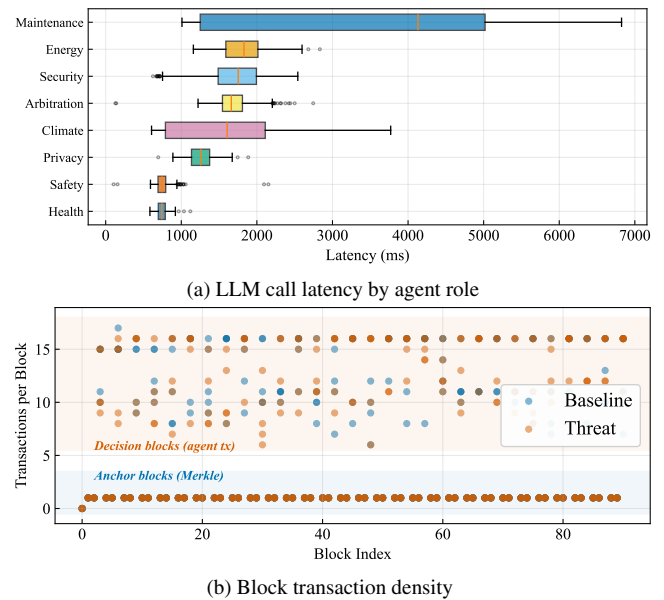


FIGURE 16: End-to-end performance profile. (a) Safety-critical agents respond fastest (median 743 ms); maintenance is slowest (median 4,131 ms). (b) Anchor blocks hold exactly 1 transaction while decision blocks carry 5–17, with both bands stable across 90 blocks.

points cluster around the 196-nonce median line from block 0 through block 90, with no upward or downward trend. Occasional spikes reaching 10^4 - 10^5 nonces appear in both conditions and at no particular block range, indicating that these outliers are a natural property of the PoW hash search rather than a response to threat-induced transaction bursts.

Fig. 15a illustrates decisions per session. All 10 sessions achieve a perfect 100% decision acceptance rate, with no rejected or dropped decisions across the entire 3,916-decision corpus. Per-session counts range from 344 (sysval-threat-04) to 418 (sysval-threat-01), and the baseline total (1,957) is nearly identical to the threat total (1,959), confirming that threat injection does not suppress or inflate the overall decision volume. Fig. 15b presents confidence by condition. Both box plots share the same median (0.90) and a similar IQR, spanning roughly 0.70 to 0.90, with whiskers extending to 0.40 (baseline) and 0.50 (threat). A single outlier at 0.30 appears in each condition. The near-identical shape confirms that the agents reason with the same level of certainty whether or not faults are present - threats change what the agents decide, not how confidently they decide. The combination of 100% acceptance across all sessions and stable confidence under threat provides the strongest evidence for decision-layer dependability. Unlike Pillar 3, where confidence varied across model variants (0.76-0.85), the system validation holds a single model constant and shows that repeated independent runs reproduce the same quality profile, ruling out session-specific anomalies.

Fig. 16a shows LLM call latency by agent. Safety-critical

agents (Health, Safety) respond fastest, with a median of 743 ms, while maintenance is the slowest, with a median of 4,131 ms; the remaining agents cluster between 1 and 2 s. The latency ordering reflects that prompt complexity agents with a narrower decision scope complete faster. Fig. 16b is the block transaction density. Two stable bands persist across all 90 blocks: anchor blocks at exactly 1 transaction (Merkle roots) and decision blocks at 5-17 transactions (agent outputs). Neither band drifts over time, and baseline and threat points intermix within the same range, confirming that the dual-pipeline architecture maintains a consistent blockchain structure under both conditions.

G. DISCUSSION

The four pillars form a layered pipeline — governance (Pillar 1) controls what agents may do, the blockchain (Pillar 2) records and protects those decisions, multi-agent evaluation confirms that the stack holds across model variants, and system validation repeats the full pipeline ten times to rule out session-specific anomalies. A failure at any layer would propagate upward, but no such failure occurs across any tested configuration.

The strongest cross-pillar finding is the safety guarantee. Pillar 1 locks six agents at fixed priorities that no slider can override. Pillar 2's Config C commits emergency blocks in 6.8 ms - 32x faster than IOTA. Pillar 3 shows the safety agent doubling its output under threat while maintaining 100% DAR across all four models. The system validation confirms this, with a reasonably high acceptance rate across 10 sessions and safety agents responding with the lowest latency. No single experiment proves safety alone, but their convergence provides layered assurance.

On feasibility, the blockchain fits within smaller memory, and the recommended LLM (Gemini 2.5 Flash) for continuous operation. The 16 tx/s throughput concession relative to distributed platforms is irrelevant at the household scale, where tens of transactions per hour are typical. Model choice matters less for correctness (99-100% DAR across all variants) and more for confidence calibration and cost — Pro offers no advantage over Flash.

Several limitations apply. Only 12 of 18 mutable parameters have validation rules (D5 gap). The evaluation uses simulated devices. A single LLM provider (Google Gemini) was tested. The threat schedule is fixed rather than adversarial. And the architecture is scoped to a single household - multi-household deployment would require a distributed blockchain and shared governance coordination not addressed here.

VI. CONCLUSION

This paper presents S5-SHB-Agent, a smart-contract-free blockchain-based framework that addresses five gaps identified across 21 surveyed blockchain-IoT systems: absent resident agency, static consensus, the lack of LLM-based multi-agent orchestration, flat permission structures, and siloed evaluation environments. Governance evaluation confirmed that the four-tier model satisfies the Society 5.0 compli-

ance dimensions at levels that no surveyed baseline achieves, with enforcement latency orders of magnitude lower than related work. Blockchain evaluation showed that adaptive Proof-of-Work reduces emergency-phase latency while sustaining competitive throughput within a memory footprint suitable for edge deployment. Multi-agent and system validation experiments confirmed consistent decision quality across model variants and threat conditions, while maintaining full blockchain integrity across all sessions. To the best of our knowledge, S5-SHB-Agent is the first framework of its kind to simultaneously address Society 5.0-oriented governance, adaptive consensus, multi-model LLM orchestration, and unified simulation-real-hybrid deployment for smart home IoT.

Three directions are prioritized for follow-on research. The multi-agent evaluation will be extended beyond Google Gemini to include additional LLM providers, and a real-device deployment using physical IoT hardware will provide reliability data under production conditions. On the governance side, the remaining mutable parameters without boundary validation will be brought to full coverage, and the fixed threat schedule will be replaced with an adversarial injection strategy to stress-test the conflict-resolution cascade under compound threats.

REFERENCES

- [1] P. Cabinet Office. [Online]. Available: https://www8.cao.go.jp/cstp/english/society5_0/index.html
- [2] A. Siriweera and I. Paik, "Autobda: Model-driven reference architecture for automated big data analysis framework," *IEEE Transactions on Services Computing*, 2025.
- [3] A. Siriweera and K. Naruse, "Survey on cloud robotics architecture and model-driven reference architecture for decentralized multi-cloud heterogeneous-robotics platform," *IEEE Access*, vol. 9, pp. 40 521–40 539, 2021.
- [4] —, "Internet of cross-chains: Model-driven cross-chain as a service platform for the internet of everything in smart city," *IEEE Consumer Electronics Magazine*, vol. 12, no. 3, pp. 85–97, 2023.
- [5] —, "Qos-aware federated crosschain-based model-driven reference architecture for iiot sensor networks in distributed manufacturing," *IEEE Sensors Journal*, vol. 23, no. 23, pp. 29 630–29 644, 2023.
- [6] K. Ramya, S. Rath, P. Venkataraman, and R. Kumar, "Cyber physical systems security: Bridging privacy, verification, intelligence, and forensics," *IEEE Access*, pp. 1–1, 2026.
- [7] F. F. Alruwaili, M. A. Alohali, N. Aljaffan, A. A. Alhashmi, A. Mahmud, and M. Assiri, "A decentralized approach to smart home security: blockchain with red-tailed hawk-enabled deep learning," *IEEE Access*, vol. 12, pp. 14 146–14 156, 2024.
- [8] S. B. Erukala, D. Tokmakov, A. D. Aguru, R. Kaluri, A. Bekyarova-Tokmakova, and N. Mileva, "An end-to-end secure communication framework for smart homes environment using consortium blockchain system," *IEEE Access*, 2025.
- [9] F. F. Alruwaili, "Blockchain-powered deep learning for internet of things with cloud-assisted secure smart home networks," *IEEE Access*, vol. 12, pp. 119 927–119 936, 2024.
- [10] A. Akram, J. Akram, A. Alabdultif, A. Anaissi, and R. H. Jhaveri, "Secure and interoperable iomt-based smart homes," *IEEE Consumer Electronics Magazine*, vol. 14, no. 4, pp. 100–105, 2025.
- [11] Y. Yang, M. Liu, Q. Zhou, H. Zhou, and R. Wang, "A blockchain based data monitoring and sharing approach for smart grids," *IEEE Access*, 2019.
- [12] A. Kharbouch, F. H. Aghdam, N. Gholipoor, and M. Rasti, "Digital-twin-6g empowered future smart grid applications," *IEEE Wireless Communications*, vol. 32, no. 3, pp. 90–97, 2025.
- [13] J. Yang, E. Rezvani, M. A. Khan, B. Heidari, H. M. Albarakati, S. Prajapat, M. Abdel-Salam, and L. Y. Po, "Qb-autoids: A blockchain-based decentralized autonomous cyberattack detection system for consumer electronics

using hybrid double q-learning and bi-lstm,” *IEEE Transactions on Consumer Electronics*, 2025.

- [14] W. Wang, K. Yu, W. Wang, C. Su, and O. Alfarraj, “Blockchain-puf fusion for privacy-preserving authentication against ai-enabled attacks in consumer iot systems,” *IEEE Transactions on Consumer Electronics*, 2026.
- [15] A. Kumar, K. Chatterjee, A. Singh, A. Kumar, and H. Aldawsari, “Privacy-preserving federated learning with blockchain auditing for consumer electronics applications,” *IEEE Transactions on Consumer Electronics*, 2026.
- [16] S. B. Khan, K. K. Raghunath, T. Mahesh, A. Alyahya, F. Asiri, and A. Al-musharraf, “Quantum-assisted cyber-forensic techniques for investigating security vulnerabilities in smart consumer electronics,” *IEEE Transactions on Consumer Electronics*, 2026.
- [17] A. Mubarak, H. Ishfaq, W. Amin, X. Shi, S. S. Duvvuri, M. A. Saleem, and K. N. Raju, “Fpga-driven secure energy routing and attack detection in decentralized microgrids with srem-based dynamic path optimization,” *IEEE Transactions on Consumer Electronics*, 2025.
- [18] S. Khan, M. Khan, M. A. Khan, M. A. Khan, L. Wang, and K. Wu, “A blockchain-enabled ai-driven secure searchable encryption framework for medical iot systems,” *IEEE Journal of Biomedical and Health Informatics*, 2025.
- [19] A. Kumar, E. Tripathi, A. K. Tripathi, H. K. Diwedi, P. S. Rathore, and A. S. Ansari, “Sbttm: epileptic seizure prediction from eeg signal using deep learning in blockchain-enabled smart healthcare monitoring with iot networking,” *Scientific Reports*, 2026.
- [20] A. M. de Morais, F. A. A. Lins, and N. S. Rosa, “Selecting consensus algorithm integrations in a dag-based blockchain for iot using genetic algorithms,” *Journal of Internet Services and Applications*, vol. 17, no. 1, pp. 55–71, 2026.
- [21] H. Xia, C. N. A. Cobblah, Q. Xia, and J. Gao, “A scalable and memory-efficient architecture for blockchain-based iot privacy and security,” *IEEE Internet of Things Journal*, 2025.
- [22] U. Arshad, A. Tubaishat, F. Alarfaj, N. Alturki, S. Anwar, and Z. Halim, “Secure ota and logging in smart devices via blockchain evaluation,” *IEEE Consumer Electronics Magazine*, 2025.
- [23] C. Jandaeng, T. Chukleang, J. Kongsen, P. Koad, and M. Thu, “Transaction fees minimization in blockchain-based home delivery system,” *IEEE Access*, vol. 12, pp. 109 197–109 209, 2024.
- [24] J. Zhu and Z. Song, “Privacy-preserving localization in smart environments: Blockchain-driven distributed target tracking,” *IEEE Transactions on Consumer Electronics*, 2025.
- [25] M. K. Jhariya, V. Dehalwar, J. Bharti, and L. Kumar, “Energy efficient transactions for blockchain networks using adaptive global best-worst particle swarm optimization,” *Scientific Reports*, 2026.
- [26] K. Guo, C. Zhan, M. Niu, X. Li, Z. Zheng, and A. Sharma, “An integrated iot and blockchain lightweight framework for secure smart cities,” *Discover Internet of Things*, vol. 6, no. 1, p. 11, 2026.
- [27] S. Fei, Z. Yan, H. Xie, and G. Liu, “Sec-e2e: End-to-end communication security in ls-hetnets based on blockchain,” *IEEE Transactions on Network Science and Engineering*, vol. 11, no. 1, pp. 761–778, 2023.
- [28] A. Siriweera, J. Rangila, K. Naruse, I. Paik, and I. Jayanada, “S5-hes agent: Society 5.0-driven agentic framework to democratize smart home environment simulation,” 2026. [Online]. Available: <https://arxiv.org/abs/2603.01554>



Technology Society IoT group.

AKILA SIRIWEERA is an associate professor at the University of Aizu. He received BSc from the University of Peradeniya, Sri Lanka. He obtained an MSc and PhD in computer science and engineering from the University of Aizu, Japan. His current research interests include Agentic AI, Big Data, Web 3.0, and system-of-systems modeling. He has received several outstanding awards in his academic and industry careers. He is an IEEE member and a TC member of the IEEE Consumer



INCHEON PAIK (Senior Member, IEEE) received the M.E. and Ph.D. degrees in electronic engineering from Korea University in 1987 and 1992, respectively. He is currently a professor with the University of Aizu, Japan. His research interests include deep learning applications, ethical LLMs, machine learning, big data science, and semantic web services. He is a member of the IEICE, IEIE, and IPSJ.



KEITARO NARUSE is a professor at the University of Aizu, Japan. He has specialized in swarm robots and applications for agricultural-robotic systems and robot interface systems in disaster responses. He works for design, DevOps, and standardized networked-distributed intelligent robot systems with heterogeneous sensors and robots. His research team has received several awards in various international robot competitions.



ISURU JAYANADA is an undergraduate student at KD University with a strong interest in Agentic AI, full-stack software development, and information technology. He has practical experience in designing and developing web and mobile applications, with a focus on creating efficient, user-centered solutions. His academic and project work reflect a commitment to advancing his technical skills and contributing to the field of computing.



JANANI RANGILA is studying at the Faculty of Information Technology at KD University, Sri Lanka, where she is completing a Bachelor of Science in Information Technology. Her research centres on the intersection of agentic AI, distributed ledger systems, and cyber-physical governance, with a focus on deploying large language model (LLM)-based multi-agent architectures in smart home environments. She contributed to the design and evaluation of agentic systems, a Society 5.0-aligned framework integrating adaptive blockchain consensus. Her broader interests span machine learning, decentralised applications (Web3), and mobile computing. She aims to continue research at the postgraduate level, exploring scalable agentic AI systems for human-centered smart environments.



VISHMIKA DEVINDI is an undergraduate student at KD University pursuing a BSc in Information Systems, with a strong interest in software quality assurance, system development. She has practical experience in designing and developing web-based applications. Her academic and project work demonstrates a commitment to strengthening her technical expertise and contributing meaningfully to the field of computing.

...